Pharmacological Research 190 (2023) 106720

Contents lists available at ScienceDirect

Pharmacological Research

journal homepage: www.elsevier.com/locate/yphrs

# An MMP-9 exclusive neutralizing antibody attenuates blood-brain barrier breakdown in mice with stroke and reduces stroke patient-derived MMP-9 activity

Yabin Ji [a,b,1], Qiang Gao [a,c,d,1], Yinzhong Ma [a,1], Fang Wang [a,c], Xixi Tan [b,e], Dengpan Song [a,c], Ruby L.C. Hoo [f], Zening Wang [g], Xin Ge [g], Hongjie Han [h], Fuyou Guo [c,*,2], Junlei Chang [a,*,2]

[a] Institute of Biomedicine and Biotechnology, Shenzhen Institute of Advanced Technology, Chinese Academy of Sciences, Shenzhen 518055, China
[b] Department of Neurology, Nanfang Hospital, Southern Medical University, Guangzhou 510515, China
[c] Department of Neurosurgery, The First Affiliated Hospital of Zhengzhou University, Zhengzhou University, Zhengzhou 450001, China
[d] Department of Neurosurgery, Tsinghua Changgung Hospital, School of Clinical Medicine, Tsinghua University, Beijing 100084, China
[e] Department of Neurology, Yangjiang People's Hospital, Yangjiang 529500, China
[f] State Key Laboratory of Pharmaceutical Biotechnology, Department of Pharmacology and Pharmacy, LKS Faculty of Medicine, The University of Hong Kong, Pokfulam, Hong Kong 999077, China
[g] Department of Chemical and Environmental Engineering, University of California, Riverside, CA 92521, USA
[h] Department of Neurosurgery, Pingdingshan Second People's Hospital, Pingdingshan 467000, China

ARTICLE INFO

*Keywords:*
MMP-9
Ischemic stroke
Intracranial hemorrhage
Antibody therapy
Blood-brain barrier

ABSTRACT

Rapid upregulation of matrix metalloproteinase 9 (MMP-9) leads to blood-brain barrier (BBB) breakdown following stroke, but no MMP-9 inhibitors have been approved in clinic largely due to their low specificities and side effects. Here, we explored the therapeutic potential of a human IgG monoclonal antibody (mAb), L13, which was recently developed with exclusive neutralizing specificity to MMP-9, nanomolar potency, and biological function, using mouse stroke models and stroke patient samples. We found that L13 treatment at the onset of reperfusion following cerebral ischemia or after intracranial hemorrhage (ICH) significantly reduced brain tissue injury and improved the neurological outcomes of mice. Compared to control IgG, L13 substantially attenuated BBB breakdown in both types of stroke model by inhibiting MMP-9 activity-mediated degradations of basement membrane and endothelial tight junction proteins. Importantly, these BBB-protective and neuroprotective effects of L13 in wild-type mice were comparable to *Mmp9* genetic deletion and fully abolished in *Mmp9* knockout mice, highlighting the *in vivo* target specificity of L13. Meanwhile, *ex vivo* co-incubation with L13 significantly neutralized the enzymatic activities of human MMP-9 in the sera of ischemic and hemorrhagic stroke patients, or in the peri-hematoma brain tissues from hemorrhagic stroke patients. Overall, we demonstrated that MMP-9 exclusive neutralizing mAbs constitute a potential feasible therapeutic approach for both ischemic and hemorrhagic stroke.

## 1. Introduction

Stroke is one of the leading causes of human disability and death globally. A stroke occurs when a cerebral blood vessel is either blocked by a clot (ischemic stroke, in most cases) or ruptures (hemorrhagic stroke). Blood-brain barrier (BBB) critically regulates the exchange of substances between neural tissue and circulation and thus maintains the homeostasis of neural microenvironment and function [1,2]. BBB breakdown can be induced by ischemia/reperfusion (I/R) injury during ischemic stroke or hemorrhage and subsequent neuroinflammation during hemorrhagic stroke [3,4]. As a result, BBB breakdown directly contributes to the hemorrhagic transformation (HT) after I/R injury, and hematoma expansion, brain edema or cerebral hernia after brain artery rupture [5–7]. Except for aggravating the outcomes of stroke,

* Corresponding authors.
*E-mail addresses:* chyou666@hotmail.com (F. Guo), jl.chang@siat.ac.cn (J. Chang).
[1] These authors contributed equally to this study.
[2] These authors jointly supervised this study and share the corresponding authorship.

https://doi.org/10.1016/j.phrs.2023.106720
Received 2 December 2022; Received in revised form 27 February 2023; Accepted 6 March 2023
Available online 7 March 2023

complications of BBB breakdown also restrain the application of treatments for acute ischemic stroke (AIS). In order to reduce risks of BBB breakdown and occurrence of HT, the "time window" of recanalization therapies after ischemic stroke is restricted within 4.5–6.0 h (h) following ischemia onset [8], which results that more than 90% patients cannot be treated by recanalization therapies [9]. Hence, BBB protection has been a promising strategy to improve both the treatment and prognosis of acute stroke patients.

The matrix metalloproteinases (MMPs) are a zinc-dependent endopeptidases family with at least 26 closely related members in humans that are involved in numerous physiological and pathological processes [10]. Of all the MMPs, MMP-9 (gelatinase B) has been intensively studied in the pathogenesis of BBB breakdown and brain cell death during the acute stage post-stroke [11–13]. Both the expression and activity of MMP-9 are rapidly upregulated a few hours after cerebral ischemia or intracranial hemorrhage (ICH), resulting in degradation of extracellular matrix, reduced tight junctions of endothelial cells and disruption of cell-matrix signaling [14–16]. In ischemic stroke models and exploratory clinical trials in patients with ischemic stroke, inhibition of MMP-9 significantly reduced BBB breakdown and neural tissue injury [14], clearly indicating a therapeutic potential of MMP-9 inhibition in ischemic stroke treatment. In contrast, the therapeutic potential of MMP-9 inhibition in ICH remains debatable and thus requires further investigation, as genetic deletion and pharmacological inhibition studies have generated inconsistent results in animal models [17–20].

All the MMP-9 chemical inhibitors developed so far were either repurposed clinically-approved drugs with unclear mechanisms and target specificities (minocycline, atorvastatin, melatonin, *etc.*), or were broad spectrum MMP inhibitors that target MMPs promiscuously (BB-1101, BB-94, GM6001, *etc.*) [14] (Table 1). SB-3CT and its water-soluble derivatives, the most-specific MMP-9 inhibitors so far, actually have higher binding affinities to MMP-2 than MMP-9 [21,22]. Therefore, a functional inhibitor that solely targets MMP-9 with clear mechanism is urgently needed to further determine the therapeutic value of MMP-9 inhibition in ICH and for the treatment of acute stroke patients.

**Table 1**
MMP-9 targeted drugs for experimental stroke treatment. IS, ischemic stroke; ICH, intracranial hemorrhage. *BB-94 showed detrimental effects in ICH model.

| Name | Specificity | Property | Stroke model and therapeutic effect |
|---|---|---|---|
| BB-1101 | Broad spectrum | Small-molecule | IS ([68]): reduced BBB damage but failed to reduce brain lesion size.<br>IS ([69]): reduced BBB damage.<br>ICH ([17]): reduced brain edema. |
| Ilomastat (GM6001) | Broad spectrum (MMP-1/−2/−3/−7/−8/−9/−12/−14/−26) | Small-molecule | IS ([70]): reduced brain tissue loss and promoted angiogenesis.<br>ICH ([18]): reduced brain injury volume and edema. |
| Batimastat (BB-94) | Broad spectrum (MMP-1/−2/−7/−9) | Small-molecule | IS ([38]): reduced ischemic lesion volume.<br>ICH ([20]): increased hemorrhage size and neuronal death* . |
| SB-3CT | MMP-2, MMP-9 | Small-molecule | IS ([32]): reduced brain infarct volume and neurological impairment. |
| MMP-9 mAb (Mouse IgG) | MMP-9 | Biologics | IS ([24]): reduced brain infarct size. Note that antibody was administered 1 h before MCAO. |
| MMP-9 mAb (Human IgG used in the current study) | MMP-9 | Biologics | IS (The current study): reduced both BBB damage and brain infarct volume.<br>ICH (The current study): reduced both BBB damage and hematoma volume. |

Monoclonal antibodies (mAbs) with high specificities and safety profiles hold great potential as therapeutic agents for many pathogenic targets including proteases. Unfortunately, there has been no any mAb drug approved for stroke treatment so far. A pioneer study reported an MMP-9 neutralizing mAb [23], which showed neuroprotective effect when prophylactically administered before permanent cerebral ischemia in rats [24]. However, the therapeutic effect of MMP-9 mAb in ischemic and hemorrhagic strokes remains unclear. L13 is an MMP-9 neutralizing human IgG mAb, which was recently developed by us using a direct inhibitory function selection strategy with nanomolar potency, exclusive specificity (no inhibition on MMP-2 or other MMPs) and biological function *in vivo* [25]. In this study, we explored the therapeutic potential of L13 in mouse models of ischemic or hemorrhagic stroke and determined its inhibitory effect on the enzymatic activity of human MMP-9 in stroke patient sera and peri-hematoma brain tissues as a model of *ex vivo* clinical trial. To the best of our knowledge, these studies for the first time provide strong preclinical and clinical support for the translational potential of MMP-9 neutralizing mAbs in acute stroke treatment.

## 2. Materials and methods

### 2.1. Animals

Male C57BL/6 mice at 8–10 weeks old and weighing 20–23 g were purchased from the Beijing Vital River Laboratory Animal Technologies Co. Ltd and housed for 1 week before being used for experiments. Homozygous B6. FVB(Cg)-*Mmp9*$^{tm1Tvu}$ (*Mmp9* knockout) mice were purchased from The Jackson Laboratory (#007084; Bar Harbor, ME). The offspring homozygous mice were produced in the experimental animal facility of Shenzhen Institute of Advanced Technology, Chinese Academy of Sciences (SIAT CAS). Only male mice were used in this study, as estrous cycle in females causes changes in estrogen levels, which lead to variations in infarct size and neurological outcomes in female animals. The detailed total number of animals in each experiment was recorded in Supplementary Table 1. Animals were kept with a 12 h light-dark border circulation system under a pathogen-free condition. All procedures for mice were approved by the Animal Care and Use Committee of SIAT, CAS. Animals were randomized for the sham operation, stroke or post-stroke treatment. The examiners were blind to the grouping or treatments of mice. For the surgery, 4% isoflurane was used to induce anesthesia in an induction chamber; 2% isoflurane was used to maintain anesthesia through a face mask (RWD, Shenzhen, China). During the entire operation, a heating pad was used to keep the core temperature of the mice at 37 ± 0.5 °C.

### 2.2. Stroke models

We used a modified intraluminal filament model to induce left middle cerebral artery occlusion (MCAO), as previously described [26]. Briefly, the left common carotid artery, internal carotid artery (ICA), and external carotid artery (ECA) were exposed *via* a midline incision in the neck, and the ECA was ligated and transected. A piece of nylon filament with a silicon tip (0.20 ± 0.01 mm; cat. #MSMC21B120PK50, RWD Life Science Co., Ltd., Shenzhen, China) was introduced into the ICA through the recurved ECA and was advanced about 10 mm beyond the carotid artery bifurcation, until a faint resistance was felt. After 60 min (min) occlusion, reperfusion was established by retracting the filament. To verify the success of MCAO surgery and reperfusion, blood flow in the left cortex supplied by the left MCA was measured using a laser Doppler flowmetry (PERIMED AB, Sweden). The mice without a decrease in blood flow at least below 30% of the baseline value after filament insertion were excluded from the study. The success of reperfusion was determined by an increase in blood flow above 70% of the baseline value

after filament retraction. In addition, the animals were further evaluated after the operation and would be removed if no neurological deficits (score = 0) were found, according to the pre-determined exclusion plan. During the entire reperfusion period, animals could get food and water at will. In the treatment of animals by sham operation, inserting nylon wire into the ICA about 5 mm away from the recurved ECA, without causing cerebral embolism, and other procedures were the same as those in ischemic mice. 48 h after the MCAO surgery, neurologic deficit score [27], grab test score [28], and horizontal ladder test score [29] were measured by researchers who were blind to the grouping and treatments of mice. The mice were followed up for seven days, and the survival rate was recorded daily.

For ICH surgery, the mice were placed on a three-dimensional precise positioning framework (Stoelting Co., Wood Dale, IL). Make an incision on the skin along the sagittal center line to expose the skull. Inject collagenase VII (sterile-filtered, 0.15 U in 0.5 μl sterile saline, Sigma, St Louis, MO) into the left basal ganglia of mice at the following stereotactic coordinates according to the punch: front 0.3 mm, 2.3 mm lateral of the bregma, and 3.8 mm in depth, apply a 1 μl microsyringe (Hamilton, Reno, NV, USA) over a period of 2.5 min at a rate of 0.2 μl/min. Leave the needle tube for another 10 min and slowly withdraw (at a rate of 1 mm/min) to minimize the flow of the introduced collagenase-saturated solution along the needle tube's trajectory. Seal the burr hole with bone wax, suture the skin surgically, and let the mice recover under observation. For the sham control mice, the equivalent sterile saline was used to replace collagenase VII. The mice that died before the scientific research were excluded; otherwise, all animals would go to the final analysis. Multiple behavioral scores [27–29] were also evaluated at 48 h post-ICH.

### 2.3. MMP-9 mAb (L13) production and treatment

L13 was synthesized as previously described [25]. Briefly, L13 heavy-chain (HC) was fused with human poliovirus internal ribosome entry site (IRES) and a downstream zeocin resistant gene by overlapping PCR, and cloned into the vector pCIW. L13 light-chain (LC) expression vector with hygromycin resistance was constructed similarly. Expi293F cells were maintained in Gibco Expi293 expression medium (Life Technology) at 37 °C and 8% CO2 with orbital shaking at 135 rpm and were transfected with HC and LC expression vectors and PEI MAX 40 K (Polysciences). After 24 h, stable cell lines were selected in fresh medium supplemented with 500 μg/ml zeocin and 350 μg/ml hygromycin for 8 days and then with 100 μg/ml zeocin and 50 μg/ml hygromycin for 15 days. For L13 IgG production, $1 \times 10^6$/ml stable cells were cultured in fresh media without antibiotics for 7 days. L13 IgG was purified from collected culture supernatant by protein A affinity chromatography. The quality of L13 IgG was confirmed by SDS-PAGE and MMP-9 inhibition assay.

L13 at doses of 1, 2.5, 5, 10 or 15 mg/kg body weight or control human IgG (#SP001, Solarbio, Beijing, China) was administered by retro-orbital i.v. injection immediately after MCAO at the onset of reperfusion or after collagenase VII injection in the ICH model. Because the *in vivo* half-life of L13 in mice was 4–5 days (data not shown), L13 was administered only once during the treatment process in both stroke models. As a comparison, SB-3CT (Selleck, Shanghai, China; Cat. #S7430; 25 mg/kg body weight) in a vehicle solution (10% DMSO in normal saline) or 10% DMSO was injected intraperitoneally at 0, 12 h, 24 h, 36 h after MCAO from the onset of reperfusion.

### 2.4. Brain infarction or hematoma analysis

48 h after reperfusion, isoflurane was used to deeply anesthetizes the animals. The whole brains were removed and cut into coronal slices (2 mm thickness) in a unique concave groove (RWD, Shenzhen, China). Brain slices were transferred into 1% 2,3,5-triphenyltetrazolium chloride (TTC, Sigma-Aldrich, St Louis, MO; Cat. #T8877), and incubated at 37 °C for 10 min. Later, the saturated TTC solution was replaced with 4% paraformaldehyde. 2 h later, a digital camera was used to take pictures, and the infarct size was measured by the ImageJ software (National Institutes of Health, US). To eliminate the effect of post-ischemic edema to the volume of injury, infarct size (%) was calibrated as described previously [30,31], and calculated as [(volume of the right hemisphere – the non-infarct volume of the left hemisphere)/volume of the right hemisphere] × 100%.

For ICH mice, the whole brains were removed and sectioned into coronal slices (2 mm thickness) in the concave groove, and the brain slices were transferred into 4% paraformaldehyde. After 2 h, the slices were photographed, and the hematoma region was accurately measured by the ImageJ software.

### 2.5. Measurement of Evans blue leakage

100 μl Evans blue (2%, Sigma-Aldrich, St Louis, MO; Cat. #E2129) or normal saline (0.9% NaCl) as the vehicle control was retro-orbitally administered and was allowed to circulate for 18 – 20 h. Then the mice were deeply anesthetized with isoflurane, and cold normal saline (15 ml/mouse) was injected into the beating heart through the left ventricle to remove the dye from the blood vessels. The brains were taken off and photographed. Then brains were separated into contralateral non-stroke and ipsilateral stroke hemispheres, and homogenized in 50% trichloroacetic acid (1 ml/hemisphere). After centrifugation (10000 rpm, 20 min), the supernatant was diluted with ethanol at a ratio of 1:4. The Evans blue concentrations were accurately determined with a fluorescence reader (stimulated at 620 nm; emission at 680 nm). The results are shown as the ratio of Evans blue content in the ipsilateral (ipsi) hemisphere to that in the contralateral (contra) hemisphere.

### 2.6. Patients

The human observational study was approved by the Ethics Committee of SIAT, CAS (No. SIAT-IRB-210315-H0556). Written informed consent was obtained from all subjects. The serum samples of ICH patients including both males and females were obtained within 72 h after stroke from The First Affiliated Hospital of Zhengzhou University (Zhengzhou, China) and Pingdingshan Second People's Hospital (Pingdingshan, China). The brain tissues around or in the hematoma from ICH patients were obtained during regular brain tissue resection procedures within 72 h after stroke at The First Affiliated Hospital of Zhengzhou University (Zhengzhou, China) with approval by the Research and Clinical Trial Ethics Committee of the First Affiliated Hospital of Zhengzhou University. The inclusion criterions were the diagnosis of hemorrhage verified by computer tomography (CT) and admitted within 24 h after symptoms onset. The serum samples of AIS patients including both males and females were obtained within 24 h after stroke from Yangjiang People's Hospital (Yangjiang, China). Patients diagnosed with AIS were consecutively recruited if they met the following criteria: (1) presented with AIS due to cerebral infarction which was confirmed by CT or magnetic resonance imaging (MRI), (2) had no intravenous thrombolysis or endovascular treatment. All patients who were aged > 18 years, with severe systemic diseases such as liver or kidney failure, coronary heart disease, hyperpyrexia, serious infection, or chronic inflammatory diseases were excluded. The control group included 3 healthy people. They were matched according to age and gender to the patient group. The exclusion criteria for the control group were the same as those described above. All samples were frozen at – 80 °C until analysis.

### 2.7. Gelatin zymography and in situ zymography

The activities of MMP-9 in brain tissue or serum samples were measured by gelatin zymography or *in situ* zymography. In gelatin zymography, brain tissues were homogenized in lysis buffer (GENMED,

Shanghai, China; Cat. #GMS30071.5) on ice and centrifuged at 10000 g for 15 min. The 10% tris gel containing 0.1% gelatin as the substrate (#ZY00102BOX, Invitrogen, Carlsbad, CA) was used to separate proteins of brain tissues or serums. The gel was then denatured and incubated in a reaction buffer (#XF-P17750, XinFan Bio-tech, Shanghai, China) at 37 °C for 24 – 48 h. Then, the gel was dyed with 0.5% Coomassie blue R-250 for 1 h and decolorization with 10% acetic acid, 50% methanol and 40% $H_2O$. The gelatinolytic activity was shown as horizontal white bands on the blue background, and the density was determined by Image J software. In the *in vitro* experiments of L13 neutralizing MMP-9 activity in serums and brain tissues of stroke patients, we added L13 to human samples in a molar ratio of 7.6:1 and incubated them at 37 °C for 90 min. The proteins in the mixed sample were then separated by 10% tris gelatin gel for zymographic analysis. Recombinant MMP-9 (rMMP-9, #50560-MNAH, Sino Biological, Beijing, China) and rMMP-2 (#10082-HNAH, Sino Biological, Beijing, China) protein was used as positive controls to pinpoint the size of endogenous MMP-9 and MMP-2, respectively.

For *in situ* zymography, the 7-μm-thick sections were cut from the fresh mouse brain embedded in OCT, and the MMP-9-*in situ* zymography kit (#GMS80062.5, GENMED, Shanghai, China) was used according to the manufacturer's instructions. Slides were mounted in antifading mounting medium with Propidium Iodide (Solarbio, Beijing, China), and imaged with an Olympus microscope to obtain 20 × images. ImageJ quantitatively analyzed the relative density of fluorescent data signals in 5–8 areas of arbitrary strokes.

### 2.8. Immunofluorescence staining

Frozen brain slices were cut into 7-μm-thick sections, which were dried on adhesion microscope slides (CITOTEST, Haimen, China) at room temperature, and rehydrated in PBS. Sections were incubated in blocking buffer containing 0.2% Triton X-100 + 10% normal goat serum in PBS at room temperature for 1 h. The following primary antibodies were diluted in PBS containing 0.2% Triton X-100 + 5% goat serum and applied to sections at 4 °C for overnight incubation: hamster anti-mouse CD31 (1:200, #MAB1398Z, Millipore, Billerica, MA), rabbit anti-laminin (1:200, #L9393, Sigma-Aldrich, St. Louis, MO), rabbit anti-collagen IV (1:100, #ab6586, Abcam, Cambridge, MA), rabbit anti-ZO-1 (1:100, #40–2200, Thermal Fisher, MA), rabbit anti-claudin-5 (1:40, #34–1600, Thermal Fisher, MA), donkey anti-mouse IgG (1:500, #715–545–150, Jackson ImmunoResearch, West Grove, PA). Slides were washed in PBS for 5 min, 3 times to remove excess primary antibodies. The following secondary fluorescently labeled antibodies were were diluted in PBS containing 0.2% Triton X-100 + 5% goat serum, applied to slides and kept at room temperature for 1 h: Alexa Fluor 488 donkey anti-rabbit IgG (1:500, #711–545–152) and Cy3 goat anti-hamster IgG (1:500, #127–165–099), both of which were from Jackson ImmunoResearch, West Grove, PA. Slides were mounted in antifading mounting medium containing DAPI (Solarbio, Beijing). An Olympus microscope was used to obtain 20 × or 40 × images. The total area or relative density of the immunofluorescence data signal was quantified and analyzed by ImageJ, and normalized according to the total capillary area (CD31 signal area) in 5–8 arbitrary stroke regions per mouse.

### 2.9. Western blotting

For the analyses of MMP-9 and the marker proteins of BBB components in the stroke regions, a 2-mm-thick coronal slice was obtained with a distance of 3.30 mm from the brain bregma. At 24 h or 48 h after the onset of stroke, brain tissues were dissected and collected. Tissues were lysed in the RIPA buffer solution (Solarbio, Beijing, China) containing protease and phosphatase inhibitors, and quantitative protein concentration analysis by BCA assay was carried out according to standard protocols. Protein lysates from every sample at equal amounts were fractionated on 10% SDS-PAGE gels and transferred onto polyvinylidene fluoride membranes. The following primary antibodies were used: rabbit anti-ZO-1 (1:1000, #40–2200, Thermal Fisher, MA), rabbit anti-occludin (1:1000, #71–1500, Thermal Fisher, MA), rabbit anti-claudin-5 (1:500, #34–1600, Thermal Fisher, MA), rabbit anti-laminin (1:1000, #L9393, Sigma-Aldrich, St. Louis, MO), rabbit anti-collagen IV (1:1000, #ab6586, Abcam, Cambridge, MA), and rabbit anti-MMP-9 (1:1000, #ab38898, Sigma-Aldrich, St Louis, MO). Normalization loading controls include β-actin (CST, MA) or albumin (Abcam, Cambridge, MA). Membranes were imaged using the GelView 6000 M system (BioLight, Zhuhai, China).

### 2.10. OGD-R

The mouse brain endothelial cells bEnd.3 (#CRL-2299, American Type Culture Collection, USA) were cultured in Dulbecco modified eagle medium (DMEM) containing 1% penicillin and 10% fetal bovine serum (FBS). Cultures were kept in a humidified incubator with 5% $CO_2$ at 37 °C, and passaged at 80 – 90% confluence. Subsequently, the cells were applied to oxygen-glucose deprivation and reperfusion (OGD-R). Briefly, the cultured medium was replaced by DMEM (D6540, Solarbio, Beijing, China) without FBS and glucose, and the cultured cells were put in a Modular Incubator Chamber (Billups-Rothenberg, MA) with 0.5 – 1% $O_2$ and 99% $N_2$, monitored by an $O_2$ analyzer (HNZA, Zhengzhou, China). Cells underwent 6-h OGD before returning to the normal culture condition. In addition, L13 or control IgG were added to the culture medium during 3 h oxygen-glucose recovery.

### 2.11. Trans endothelial electric resistance (TEER) and BBB permeability measurements

We used the Millicell-ERS-2 (Millipore, Germany) to accurately measure TEER. bEnd.3 cells were seeded at a density $1.5 \times 10^4$ per well on the 0.4 μm pore size Transwell permeable membranes (24-well cell culture inserts; Costar, Corning, NY) and grew for 3 days before use. TEER measured before OGD-R treatment was set as the baseline and TEER values measured in the vacant Transwell filters were subtracted for normalization. Endothelial monolayer permeability to 70 kDa FITC-dextran (Sigma-Aldrich, St. Louis, MO) was measured after OGD-R to assess the effect of L13. FITC-dextran at the concentration of 5 ug/ml was added to the luminal compartment of each insert (10 μl). 30 min later, 100 μl medium was taken from the abluminal chamber and the fluorescence was measured at 520 nm with a fluorescence plate reader (MULTISKAN GO, Thermo scientific, MA). Additionally, the effect of L13 with 200 or 500 nM for endothelial injury induced by rMMP-9 protein with 100 nM for 2 h was also investigated.

### 2.12. Statistical analysis

The SPSS 20.0 for Windows software package was used for statistical analysis. Data were expressed as means ± standard error (SE). Unpaired Student's *t*-test was used to compare two groups. Paired Student's *t*-test was used for samples of patients with L13 or control IgG treatment. One-way analysis of variance (ANOVA) was used to determine statistical differences of all observation index values from the different groups. The Least Significant Difference (LSD) *t*-test or the Dunnett T3 test, if the variance was heterogeneous, was used to further analyze differences. Statistical significance was defined as $P < 0.05$.

## 3. Results

### 3.1. MMP-9 mAb L13 attenuated brain tissue injury and improved the neurological outcomes of mice following ischemic stroke

The MMP-9 mAb L13 was functionally selected using the catalytic domain of human MMP-9 [25], which is highly conserved in mouse

MMP-9 with 92.7% similarity. Therefore, we firstly determined the therapeutic efficacy of L13 in a mouse model of ischemic stroke. After 1 h-ischemia and 48 h-reperfusion, extensive infarction was detected in the cortex and subcortex of sliced brain sections, and single time retro-orbital injection of L13-IgG with a dose of 2.5 and 5 mg/kg, but not 1 mg/kg, significantly decreased the infarct volumes to 25.3 ± 2.0% and 21.1 ± 1.5%, respectively, as compared with the control IgG group (31.4 ± 1.7%; F =4.842, $P = 0.019$ and $P < 0.001$, respectively), as revealed by TTC staining (Fig. 1B, C). We also determined the effect of higher doses of L13 (10 mg/kg and 15 mg/kg) on infarct volume in another independent experiment, but no further neuroprotection was found (Supplementary Fig. 1), suggesting that 5 mg/kg was the most effective dose of L13-IgG in our stroke model. L13-IgG treatment decreased the neurological deficit scores ($t = 3.000$, $P = 0.0077$) and improved the grab ($t = 3.536$, $P = 0.0024$) and horizontal ladder ($t = 4.799$, $P = 0.0001$) movements of mice with MCAO/reperfusion (MCAO/R; Fig. 1D). Results in the seven days survival assay showed that 45% mice (8 of 18) in the control IgG group were survived at day 7, which was much lower than that in the L13-IgG group (75%, 13 of 17; $P < 0.01$; Fig. 1E). Taken together, these results show that L13 treatment at the onset of reperfusion rendered better outcomes of ischemic stroke in short and long terms.

In order to evaluate the efficacy of L13 in comparison with currently available MMP-9 inhibitors, we compared the neuroprotective effects of L13 with SB-3CT, a small molecule inhibitor of MMP-2 and MMP-9 widely used in animal stroke model studies [32,33], in mice with 1 h-MCAO and 48 h reperfusion. As expected, SB-3CT also significantly reduced the infarct volume (F = 4.842; $P = 0.017$) and improved

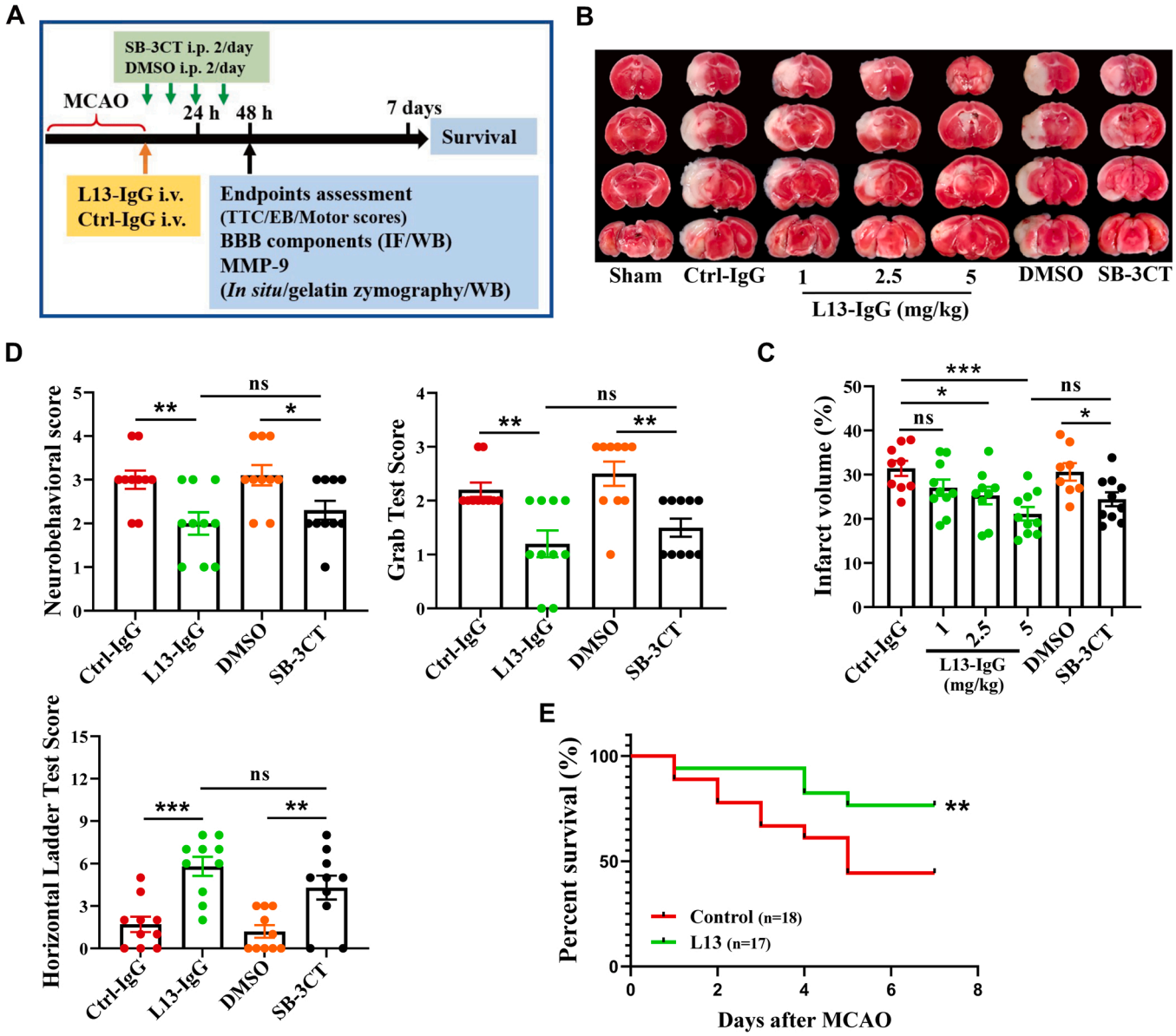


**Fig. 1. MMP-9 mAb (L13-IgG) improved the stroke outcomes in adult mice with ischemic stroke.** (A) Experimental procedure. (B) TTC staining of coronal brain tissue slices after 1 h-MCAO and 48 h-reperfusion. Infarcted areas were visualized as white in TTC staining. (C) Quantifications of infarct volume as determined by TTC staining in mice treated with control human IgG, L13-IgG (1, 2.5 and 5 mg/kg), 10% DMSO, or SB-3CT (25 mg/kg in 10% DMSO) after 1 h-MCAO and 48 h-reperfusion. n = 8 – 10 mice per group. Dose of 5 mg/kg L13-IgG was chosen for the following experiments. (D) The scores of neurological deficits, grab test, and horizontal ladder test were determined in mice with L13-IgG (5 mg/kg), SB-3CT (25 mg/kg) or controls treatment following 1 h-MCAO and 48 h-reperfusion. n = 10 mice per group. (E) Survival rate of mice with L13-IgG (5 mg/kg) or control human IgG treatment during seven days of reperfusion after 1 h-MCAO. n = 17 – 18 mice per group. * $P < 0.05$, * * $P < 0.01$ and * ** $P < 0.001$. MCAO, middle cerebral artery occlusion; DMSO, dimethyl sulfoxide; TTC, 2,3,5-triphenyltetrazolium chloride; EB, Evans blue; BBB, blood-brain barrier; IF, immunofluorescence; WB, Western blot; ns, no significance.

behavioral defects (the neurological deficit scores, $t = 2.530$, $P = 0.0210$; the grab test, $t = 3.536$, $P = 0.0024$; the horizontal ladder test, $t = 3.254$, $P = 0.0044$) in mice. Furthermore, there was no significant difference in the neuroprotective effects between SB-3CT and L13 (infarct volume, F = 4.842; $P = 0.180$; the neurological deficit scores, F = 5.432, $P = 0.7926$; the grab test, F = 9.211, $P = 0.7108$; the horizontal ladder test, F = 11.57, $P = 0.3605$).

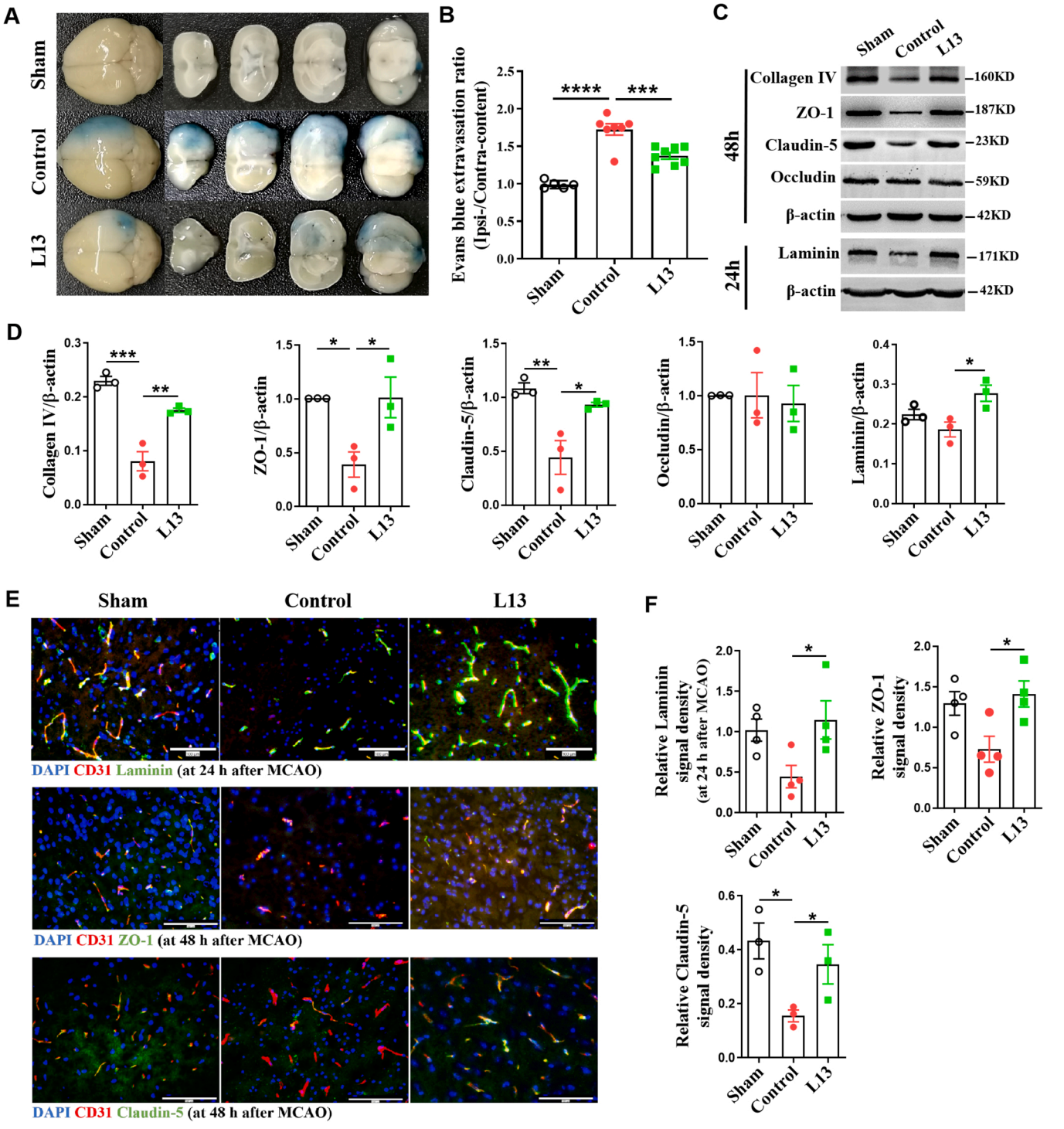


**Fig. 2. MMP-9 mAb (L13) attenuated the BBB breakdown by regulating basement membrane and endothelial tight junctions following ischemic stroke.** (A) Representative images of brains showing Evans blue leakage in MCAO/R mice by L13 or control IgG treatment with the dosage of 5 mg/kg. (B) Evans blue leakage quantification. n = 5 – 8 mice per group. (C) Detection of the basement membrane components (collagen IV and laminin) and endothelial tight junction (ZO-1, claudin-5 and occludin) protein levels in the ischemic hemisphere of mice by Western blot. (D) Quantification of the protein bands in (C). n = 3 mice per group. (E) Co-immunofluorescence staining for laminin, ZO-1, claudin-5 (green) with CD31 (red) in infarcted brain tissues. (F) Protein fluorescence signal densities were quantified and normalized to the CD31 signal area. n = 3 – 4 mice per group. 5 – 8 random low-power fields per mouse were selected. Scale bar, 100 μm. * $P < 0.05$, * * $P < 0.01$ and * ** $P < 0.001$, * ** * $P < 0.0001$. MCAO/R, middle cerebral artery occlusion/reperfusion; BBB, blood-brain barrier.

### 3.2. MMP-9 mAb L13 attenuated BBB breakdown by regulating basement membrane and endothelial tight junctions following ischemic stroke

We assessed the extent of BBB breakdown in the ischemic hemisphere by measuring the Evans blue leakage. The results demonstrated that after cerebral ischemia and reperfusion, both the injected Evans blue and human IgG proteins showed widespread extravasation into the injured brain tissue (Fig. 2 A, B and Supplementary Fig. 2), indicating substantial BBB breakdown. We further revealed that Evans blue leakage was significantly decreased in the mice treated by L13 with the dose of 5 mg/kg compared with the control mice (by 20.4%, F =37.39, $P = 0.0006$; Fig. 2 A, B). In line with the improved BBB integrity, we

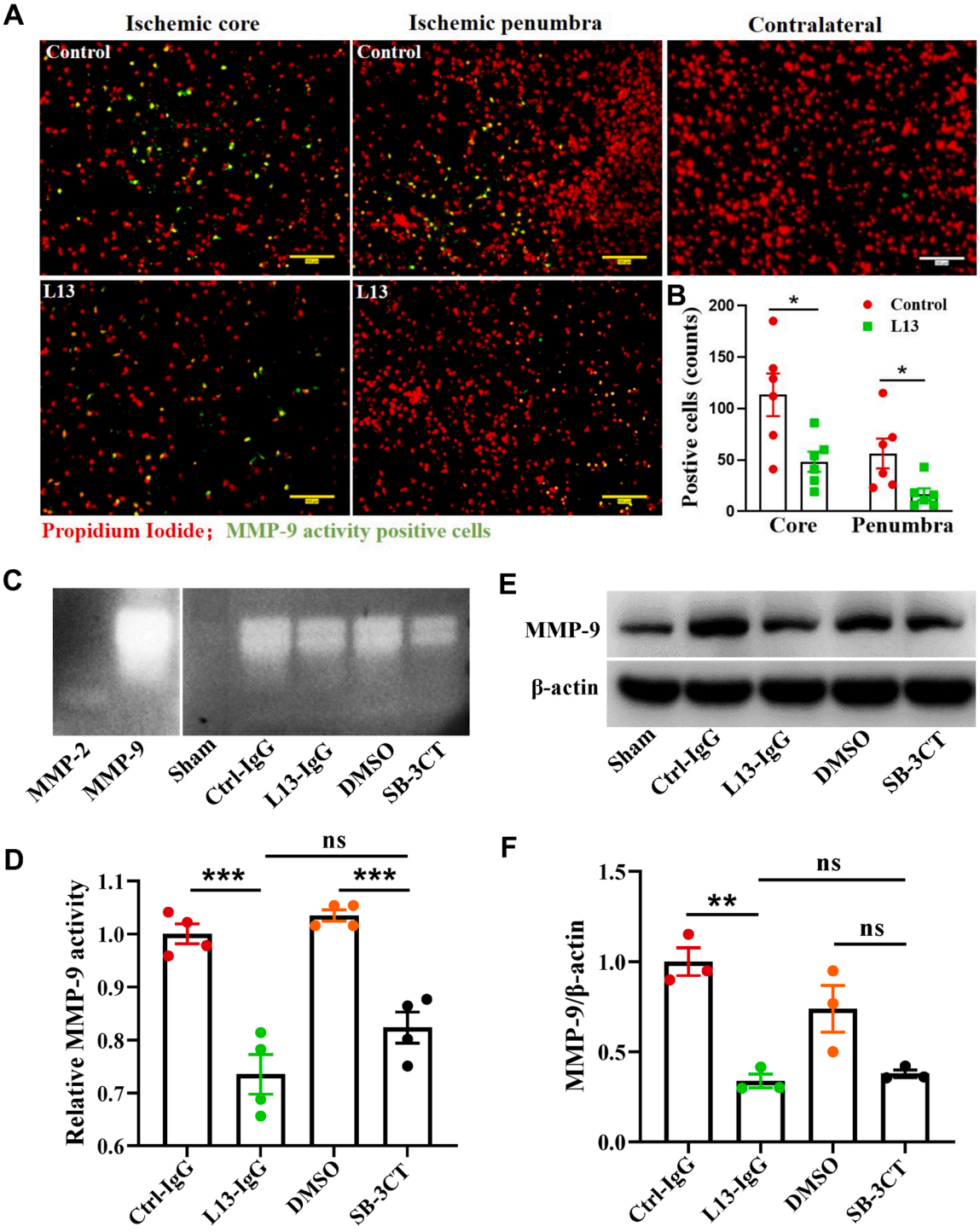


**Fig. 3. MMP-9 mAb (L13) efficiently inhibited the enzymatic activity of MMP-9 in mouse ischemic brain tissues.** (A) *In situ* zymography of MMP-9 fluorogenic substrate DQ-gel (green) merged with nuclear DNA staining by propidium iodide (red) in ischemic core and penumbra of mice with L13 or control IgG treatment after MCAO/R. Scale bar, 100 μm. (B) Quantification of MMP-9 activity positive cells. n = 6 mice per group. 5 – 8 random low-power fields per mouse were selected. (C) Gelatin zymography of MMP-9 enzymatic activity in ischemic mouse brain tissues. (D) The relative fold changes in MMP-9 activity normalized to the values in sham group. n = 4 mice per group. (E) Western blot analysis of the MMP-9 protein levels in the brain tissues of the ischemic hemisphere. (F) Quantification of the protein bands in (E). n = 3 mice per group. * $P < 0.05$, * * $P < 0.01$ and * ** $P < 0.001$. MCAO/R, middle cerebral artery occlusion/reperfusion; DMSO, dimethyl sulfoxide; ns, no significance.

observed that brain microglia activation (Iba-1-positive cells) and peripheral immune cell infiltration (CD45-positive and Ly6G-positive cells) were significantly reduced in the penumbra area of the ischemic hemispheres from mice treated by L13 (Supplementary Fig. 3). To further identify downstream effectors underlying BBB-protection of L13 after ischemic stroke, we examined components of the BBB, including endothelial tight junctions (ZO-1 and claudin-5) and basement membrane (collagen IV and laminin). After MCAO/R, the ischemic hemisphere in mice showed significantly reduced ZO-1 ($F = 7.758$, $P = 0.0340$) and claudin-5 ($F = 12.33$, $P = 0.0075$) protein levels compared with mice with sham-operation, and L13 treatment reversed the reduction ($P = 0.0256$, $P = 0.0320$; Fig. 2 C, D). Consistently, more ZO-1 ($F = 5.509$, $P = 0.0308$) and claudin-5 ($F = 4.288$, $P = 0.0489$) coverage on blood vessels was observed in infarct areas of the mice with L13 treatment than that of the control mice (Fig. 2E, F). Meanwhile, decreased collagen IV and laminin protein levels after MCAO/R were reversed by L13 treatment ($F = 42.15$, $P = 0.0029$; $F = 6.747$, $P = 0.0248$; Fig. 2 C, D), and consistent expression of laminin in immunofluorescence staining was also observed ($F = 5.943$, $P = 0.0231$; Fig. 2E, F). Taken together, our results demonstrate that L13 protected BBB integrity after ischemic stroke through regulation of the endothelial tight junctions and basement membrane.

### 3.3. *MMP-9 mAb L13 inhibited the enzymatic activity of MMP-9 in mouse ischemic brain tissues*

To determine whether administration of L13 inhibited the gelatinolytic activity of MMP-9 after ischemic stroke, we used *in situ* zymography together with propidium iodide counterstaining in the mice with MCAO/R. We compared the gelatinolytic activity of MMP-9 in the brain ischemic core and penumbra regions of mice treated with L13 *versus* control IgG. Results showed L13 abrogated MMP-9 gelatinolytic activity (core, $t = 2.845$, $P = 0.0174$; penumbra, $t = 2.574$, $P = 0.0277$; Fig. 3 A, B). Consistently, gelatin zymography and Western blot assays demonstrated that the MMP-9 activity ($t = 6.296$, $P = 0.0007$) and protein level ($t = 7.685$, $P = 0.0015$) were significantly reduced in

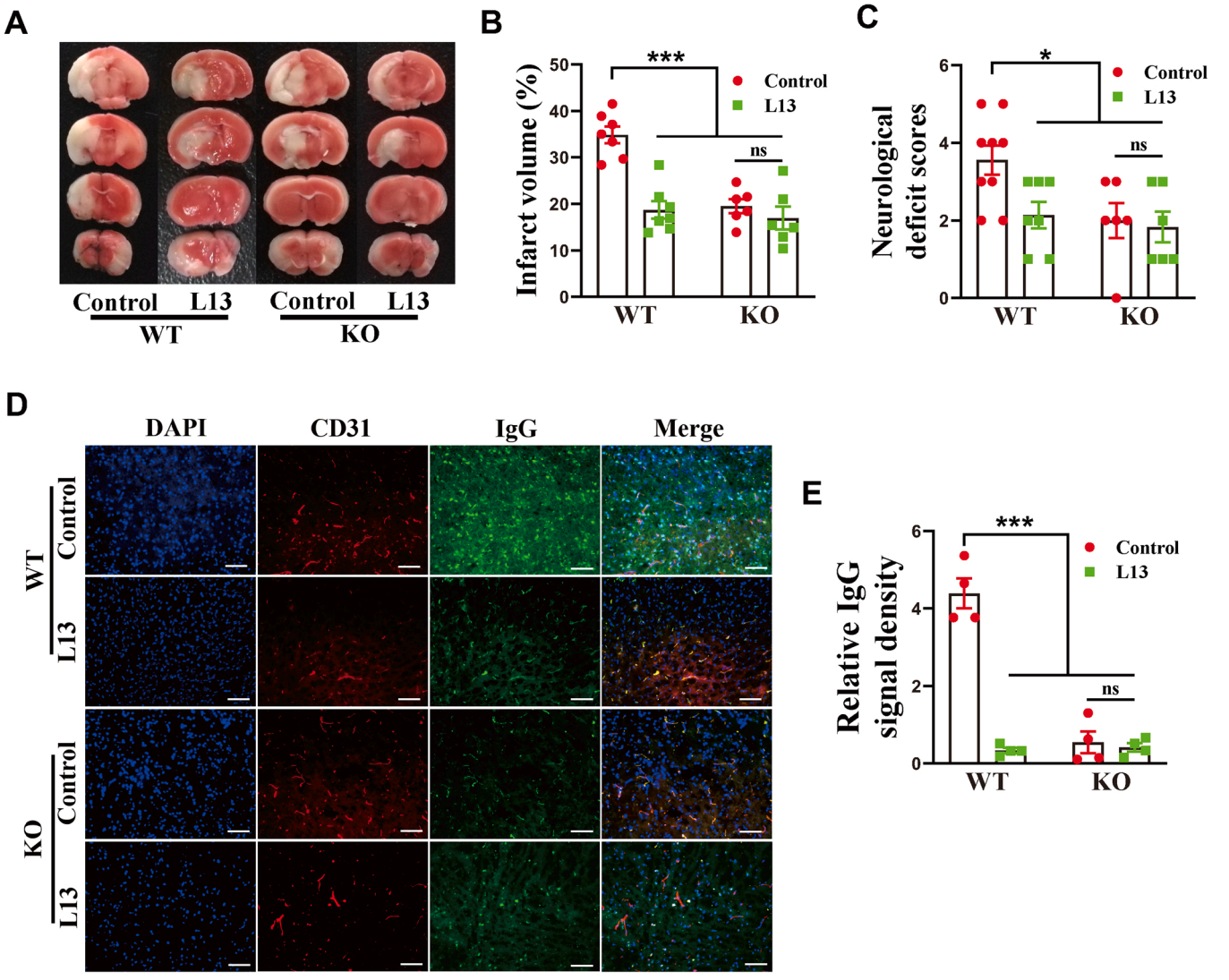


**Fig. 4. The therapeutic effect of MMP-9 mAb (L13) was abolished in *Mmp9* knockout mice with ischemic stroke.** (A) TTC staining of coronal brain tissue slices of mice with L13 or control human IgG (5 mg/kg) treatment after 1 h-MCAO and 48 h-reperfusion. Infarcted areas were visualized as white in TTC staining. (B) Infarct size was determined by TTC staining and quantified. n = 6 – 7 mice per group. (C) The neurologic deficit scores in WT and KO mice with MCAO/R-48 h after L13 or control human IgG treatment. n = 6 – 9 mice per group. (D) Co-immunofluorescence staining of endogenous plasma IgG (green) leaked from blood vessels (CD31, red) after MCAO/R-48 h in WT and KO mice with L13 or control IgG treatment. Scale bar, 100 μm. (E) Plasma IgG leakage quantification. IgG signals were normalized by CD31 signal area. n = 4 mice per group. * $P < 0.05$, * * $P < 0.01$ and * ** $P < 0.001$; ns, no significance. MCAO/R, middle cerebral artery occlusion/reperfusion; WT, wild type; KO, knockout; ns, no significance.

ischemic hemisphere after L13 treatment (Fig. 3C-F). Meanwhile, we observed that SB-3CT significantly inhibited the MMP-9 activity ($t = 6.757$, $P = 0.0005$), but not MMP-9 protein level ($t = 2.733$; $P = 0.0523$). However, there was no statistical difference between L13 and SB-3CT in inhibition of MMP-9 activity ($F = 29.69$; $P = 0.1338$) and protein level ($F = 15.91$; $P = 0.9826$) in ischemic brain tissues.

In order to further confirm the inhibition specificity and efficiency of L13 for MMP-9, we observed the therapeutic effect of L13 for the *Mmp9* KO mice with MCAO/R. Our results showed L13 had no further improvement for the brain injury ($F = 19.01$, $P = 0.9201$), neurological deficit ($F = 4.658$, $P = 0.9495$) and IgG leakage ($F = 64.78$, $P = 0.9953$) in *Mmp9* KO mice (Fig. 4A-E), supporting the protective effect of L13 for ischemic stroke resulted from the inhibition of MMP-9 activity. Additionally, we observed the better neurological outcomes in KO mice than that of wild type (WT) mice (infarction, $P < 0.0001$; neurological deficit, $P = 0.0419$; IgG leakage, $P < 0.0001$), and there was no apparent difference of the outcomes of MCAO/R between KO mice and WT mice with L13 treatment ($P > 0.05$; Fig. 4A-E), indicating that the protective effects of L13 on ischemic stroke through transiently inhibiting MMP-9 activity was comparable to that seen in mice with *Mmp9* genetic deletion. In summary, our results indicate that L13 improved the outcomes of ischemic stroke through efficient and specific inhibition of MMP-9.

### 3.4. MMP-9 mAb L13 reduced BBB disruption induced by exogenous rMMP-9 or OGD-R injury in vitro

The endothelial cell is the main component of the BBB, and it is the determinant for the barrier property of BBB. To determine the effect of L13 treatment on the integrity and barrier function of endothelial cell directly, we employed a transwell system to build the monolayer BBB. On one hand, we found exogenous rMMP-9 at 100 nM for 2 h treatment reduced the TEER value ($F = 9.909$, $P = 0.0033$) and increased the permeability ($F = 8.095$, $P = 0.0032$) of endothelial cells, but L13 at 200 or 500 nM can significantly normalize the abnormal barrier function (TEER, $P = 0.0233$; fluorescein isothiocyanate-conjugated (FITC)-

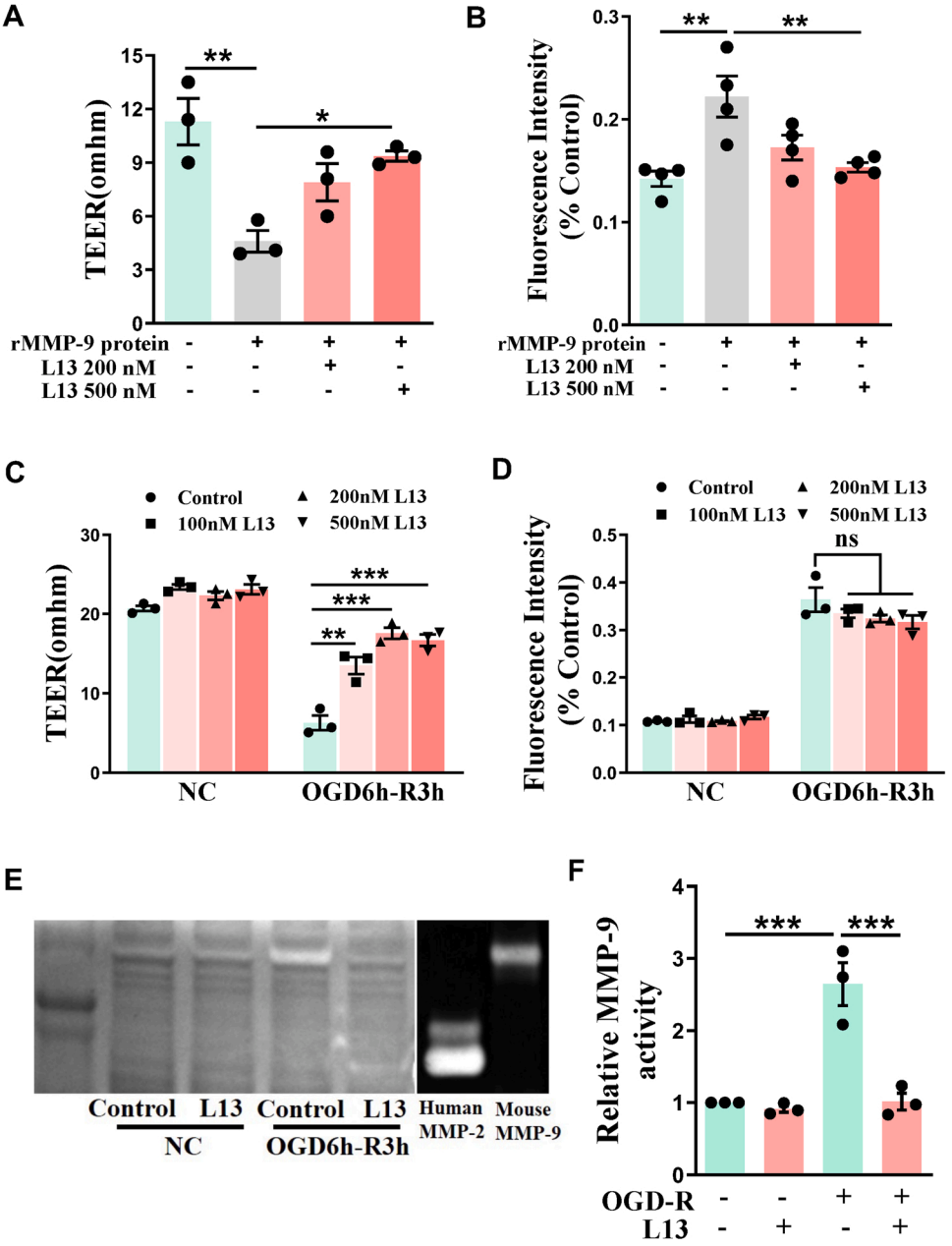


**Fig. 5. MMP-9 mAb (L13) reduced BBB disruption caused by rMMP-9 protein treatment or OGD-R injury *in vitro*.** (A) The mouse brain endothelial cells (bEnd.3) were seeded on the transwell inserts, and TEER values were measured after 2 h-treatment of 100 nM rMMP-9 protein, in the presence or absence of L13 or control IgG co-incubation. n = 3 biological replicates per group. (B) The 5 μg/ml FITC-dextran-70 kD was added into the upper chamber with bEnd.3 cells after 2 h-treatment of 100 nM rMMP-9 protein with or without L13 co-incubation. The fluorescence intensity values in the lower chamber were measured at 520 nm. n = 4 biological replicates per condition. (C) The TEER was measured without or with OGD6h-R3h, in the presence or absence of 2-h L13 or control IgG co-incubation. n = 3 biological replicates per group. (D) The fluorescence intensity of FITC-dextran-70 kD in the lower chamber were measured at 520 nm. n = 3 biological replicates per group. (E) Gelatin zymography of MMP-9 enzymatic activity in bEnd.3 cells after OGD6h-R3h, in the presence or absence of 2-h L13 or control IgG co-incubation. (F) The relative fold changes in MMP-9 activity accepting the normal control values. n = 3 samples per group. * $P < 0.05$, * * $P < 0.01$ and * ** $P < 0.001$. rMMP-9, recombinant MMP-9; OGD-R, oxygen-glucose deprivation and recovery; NC, normal condition; TEER, trans-endothelial electrical resistance.

dextran-70 kDa permeability, $P = 0.0096$; Fig. 5 A, B). On the other hand, we assessed the effect of L13 for BBB injury following OGD-R. Our results showed that in normal control, L13 had no apparent influence for endothelial cell barrier functions ($F = 6.4429$, $P > 0.05$); after OGD-R, TEER and BBB permeability value were significantly disturbed, and the decreased TEER values were apparently reversed by L13 treatment ($F = 35.53$; 100 nM, $P = 0.0016$; 200 nM, $P < 0.0001$; 500 nM, $P = 0.0001$; Fig. 5 C). Interestingly, the leakage of FITC-dextran-70 kDa was not significantly decreased by L13 treatment ($F = 1.741$, $P > 0.05$; Fig. 5D), suggesting other mechanisms such as endothelial transcytosis also contributed to the leakage of dextran under OGD-R [34]. Additionally, gelatin zymography assays demonstrated that increased MMP-9 activity after OGD-R were completely eliminated *via* L13 treatment ($F = 26.72$, $P = 0.0005$; Fig. 5E, F). Taken together, our *in vitro* data indicate that BBB injury caused by exogenous rMMP-9 or OGD-R can be effectively reduced by L13 treatment through direct protection of L13 on endothelial cells without supports from other structures of BBB.

### 3.5. MMP-9 mAb L13 improved the neurological outcomes of mice with ICH

In adult mice subjected to ICH, the crimson hematoma was detected in sliced brain sections, and single time retro-orbital i.v. injection of L13 at a dose of 5 mg/kg significantly reduced the hematoma volumes to 12.4 ± 0.8%, compared with the control group (19.8 ± 1.5%; $F = 67.04$, $P = 0.0003$; Fig. 6A-C). L13 treatment decreased the neurological deficit scores ($F = 100.2$, $P < 0.0001$) and improved the grab ($F = 17.91$, $P = 0.0036$) and horizontal ladder ($F = 88.00$, $P < 0.0001$) movements (Fig. 6D). Moreover, the extent of BBB disruption in the hematoma hemisphere, demonstrated by Evans blue ($F = 12.52$, $P = 0.0102$; Fig. 6E, F) and IgG ($F = 46.77$, $P = 0.0010$; Fig. 6 G, H) extravasation, was significantly attenuated in the mice treated by L13 at the dosage of 5 mg/kg compared with the control mice.

Consistent with ischemic stroke, after ICH, the hematoma hemisphere in mice showed significantly decreased collagen IV ($F = 12.9$, $P = 0.0069$), ZO-1 ($F = 5.843$, $P = 0.0417$), claudin-5 ($F = 24.24$, $P = 0.0011$) and occludin protein ($F = 5.650$, $P = 0.0078$) levels compared with the mice with sham-operation, and L13 treatment reversed the decreases (collagen IV, $P = 0.0221$; ZO-1, $P = 0.0215$;

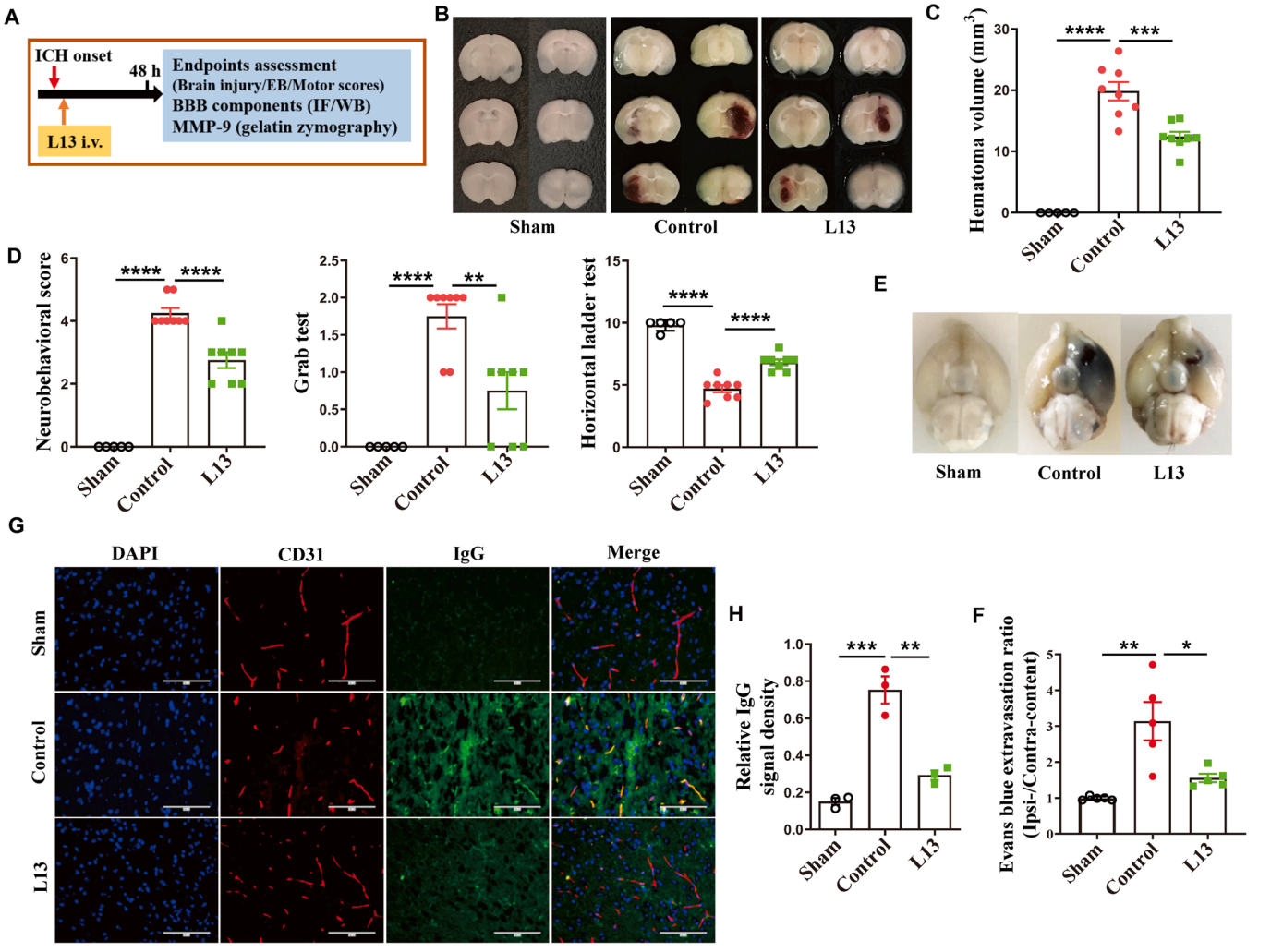


**Fig. 6. MMP-9 mAb (L13) improved the neurological outcomes in mice with ICH.** (A) Experimental procedure. (B) The hematoma volume in mice with ICH after 5 mg/kg L13 or control IgG treatment. (C) Quantification of hematoma volume of mice. n = 5 – 8 mice per group. (D) The scores of neurological deficits, grab test, and horizontal ladder test were determined in mice with ICH after L13 or control IgG treatment. n = 5 – 8 mice per group. (E) Representative images of brains showing Evans blue leakage in mice with ICH after 5 mg/kg L13 or control IgG treatment. (F) Fluorescence quantitation of Evans blue. n = 5 mice per group. (G) Co-immunofluorescence staining of endogenous plasma IgG (green) leaked from the blood vessels (CD31, red) in peri-hematoma brain tissues of mice with ICH after 5 mg/kg L13 or control IgG treatment. Scale bar, 100 μm. (H) Quantification of plasma IgG leakage. IgG signals were normalized by CD31 signal area. n = 3 mice per group. * $P < 0.05$, * * $P < 0.01$, * ** $P < 0.001$ and * *** * $P < 0.0001$. ICH, intracranial hemorrhage; EB, Evans blue; IF, immunofluorescence; WB, Western blot.

claudin-5, $P = 0.0305$; occludin, $P = 0.0486$) (Fig. 7 A, B). Meanwhile, more collagen IV ($F = 57.13$, $P < 0.0001$), ZO-1 ($F = 62.62$, $P = 0.0006$) and claudin-5 ($F = 37.73$, $P = 0.0091$) coverage on blood vessels was observed around the hematoma of the mice with L13 treatment than that of the control mice (Fig. 7 C, D). We also observed the effect of L13 for MMP-9 activity around hematoma and our results showed L13 almost eliminated MMP-9 gelatinolytic activity in gelatin zymography compared with that of control mice ($t = 2.802$, $P = 0.0487$; Fig. 7E, F). Taken together, our results demonstrate that L13 improved the outcomes of ICH and protected BBB through MMP-9 inhibition.

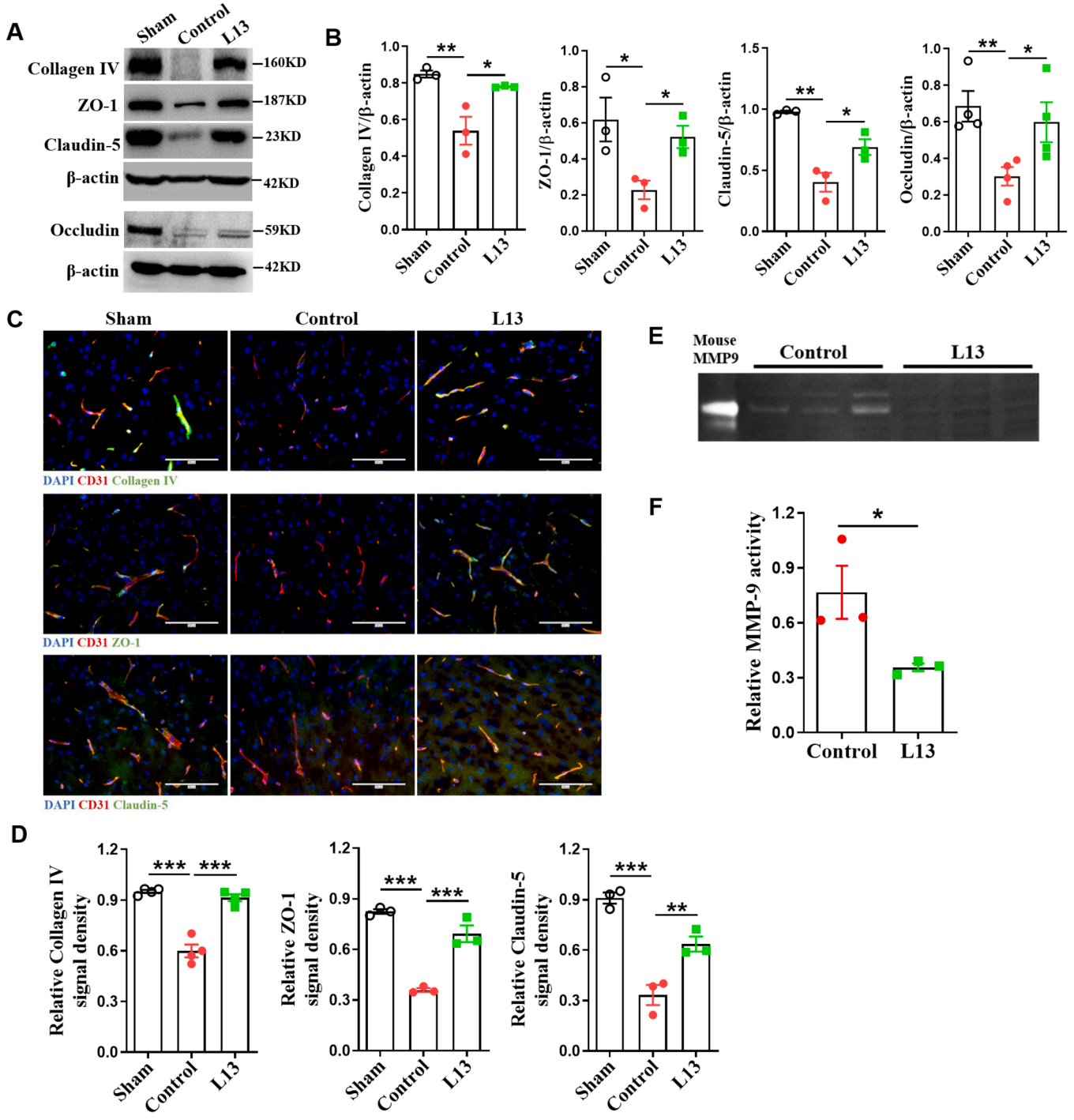


**Fig. 7. MMP-9 mAb (L13) protected basement membrane and endothelial tight junctions *via* inhibiting MMP-9 activity following ICH.** (A) The basement membrane (collagen IV) and endothelial tight junction (ZO-1, claudin-5 and occludin) protein levels in brain regions around the hematoma were measured by Western blot. (B) Quantification of the protein bands in (A). n = 3 – 4 mice per group. (C) Co-immunofluorescence staining for collagen IV, ZO-1, claudin-5 (green) with CD31 (red) in brain regions around the hematoma. The yellow signals showed double-positive signals on blood vessels. (D) Protein fluorescence signal densities were quantified and normalized to the CD31 signal area. n = 3 – 4 mice per group. 5 – 8 random low-power fields per mouse were selected. Scale bar, 100 μm. (E) Gelatin zymography of MMP-9 enzymatic activity in brain tissues around the hematoma. Recombinant mouse MMP-9 protein was used as positive control to pinpoint the size of endogenous MMP-9. (F) The relative fold changes in MMP-9 activity compared to the values in the control group. n = 3 mice per group. * $P < 0.05$, * * $P < 0.01$ and * ** $P < 0.001$. ICH, intracranial hemorrhage.

### 3.6. MMP-9 mAb L13 neutralized the enzymatic activity of human MMP-9 in stroke patient-derived samples ex vivo

Next, we determined the effect of L13 on human MMP-9 activity in serum and brain tissue samples from stroke patients *ex vivo*. The general information of patients was shown in Supplementary Table 2. Consistent with previous studies [35], serum MMP-9 protein in ICH patients was significantly higher than that in healthy people ($t = 7.950$, $P = 0.0014$; Fig. 8 A, B), but this phenomenon was not found in samples of AIS patients without reperfusion ($t = 0.7763$, $P = 0.4809$; Fig. 8 A, B). Gelatin zymography showed that MMP-9 activity in serum samples of patients with AIS ($t = 5.169$, $P = 0.0067$; Fig. 8 C, D) or ICH ($t = 5.807$, $P = 0.0011$; Fig. 8 C, D) was significantly decreased after L13 co-incubation *ex vivo*. Further, we demonstrated that L13 substantially reduced the MMP-9 activity in the peri-hematoma brain tissues collected from ICH patients that received conventional medical treatment in the acute phase [36] and surgical removal of the hematoma ($t = 3.110$, $P = 0.0144$; Fig. 8E, F). Taken together, our data showed that L13 can neutralize MMP-9 in serum and brain tissue samples of stroke patients, which provides strong evidence supporting the clinical potential of L13 for acute stroke treatment.

## 4. Discussion

MMP-9 belongs to the family of zinc- and calcium-dependent endopepidases [37], and plays important roles in the physiology and pathology of brain. In physiology, MMP-9 participates in synaptic and cortical plasticity, learning and memory, neurogenesis and so on; during pathologies, MMP-9 is involved in many brain disorders, such as stroke, multiple sclerosis, brain trauma, Alzheimer's disease and so on, and the therapeutic effects of MMP-9 pharmacological inhibition or genetic deletion have been reported in various brain disease models [14,15]. Here, we identified the therapeutic effects of a recently developed MMP-9-targeted neutralizing mAb on acute stroke, and the mechanisms underlying its BBB- and neuro- protective actions. Our data provide strong evidence supporting the therapeutic potential of MMP-9 neutralizing mAbs for acute stroke treatment by attenuating MMP-9 activation-mediated BBB breakdown.

Targeted inhibition of MMP-9 for BBB protection during acute stroke has the following advantages. First, the role of MMP-9 in BBB disruption following ischemic stroke has been established for decades with abundant of clinic and animal study evidence [14,35]. Second, although MMP-9 is involved in certain central nervous processes, no major neurological deficits and limited survival time were observed in *Mmp9* KO mice (from mouse datasheet of Jackson Laboratory) [38], which suggests MMP-9 inhibition possesses a high safety profile, especially

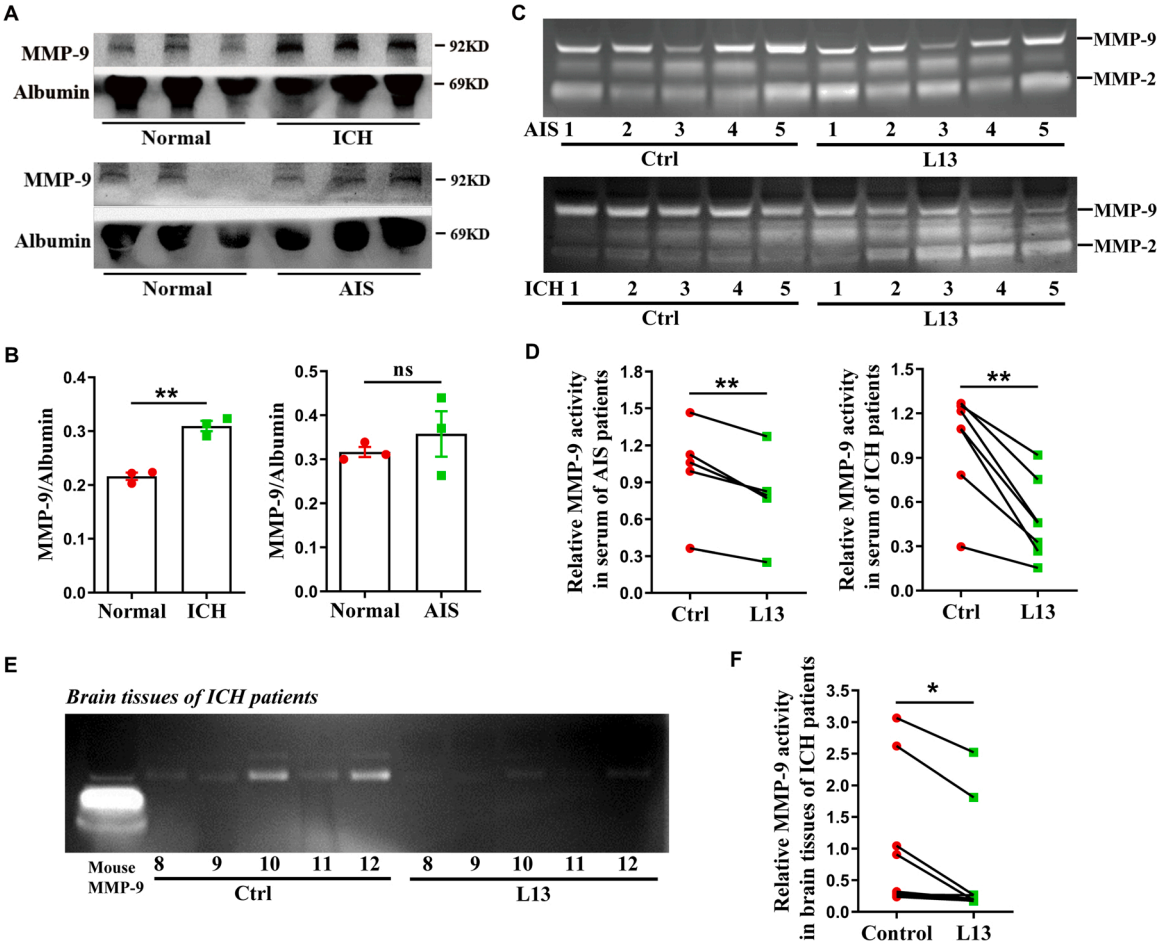


**Fig. 8. MMP-9 mAb (L13) neutralized the enzymatic activity of human MMP-9 in stroke patient-derived samples *ex vivo*.** (A) The MMP-9 protein levels in serums of stroke patients and healthy control subjects were measured by Western blot. (B) Quantitation of the protein bands in (A). n = 3 people per group. (C) Gelatin zymography of MMP-9 enzymatic activity in serums of stroke patients with co-incubation with L13 or control IgG (1:7.6, 37 ℃, 90 min). (D) The relative fold changes in MMP-9 activity compared to the values in the control group. n = 5 patients in AIS group and 7 patients in ICH group, respectively. (E) Gelatin zymography of MMP-9 activity of brain tissues around or in the hematoma. (F) The relative fold changes in MMP-9 activity compared to the values in the control group. n = 7 patients per group. * $P < 0.05$, * * $P < 0.01$. AIS, acute ischemic stroke; ICH, intracranial hemorrhage; ns, no significance.

short-term inhibition in the acute stage of stroke. Third, MMP-9 mediated BBB disruption is a common mechanism in a series of brain diseases so that MMP-9 inhibition has a potential of being a versatile strategy for BBB protection. Therefore, given the high translational potential, MMP-9 is one of the most appealing targets for protecting BBB in the acute stroke. The previous study had shown that L13 exclusively inhibited the activity of MMP-9 but not MMP-2/− 12/− 14, and had a therapeutic effect on neuropathic pain in mice [25]. Here, our data showed that the BBB protection of L13 was fully abolished in *Mmp9* KO mice, and the protective effects of L13 on ischemic stroke through transiently inhibiting MMP-9 activity was comparable to that seen in mice with *Mmp9* genetic deletion, indicating that L13 alleviates ischemic stroke through efficient and specific inhibition of MMP-9.

Until now, nearly 30 agents and methods have shown a possible or verified effect to inhibit MMP-9, but the majority of them are non-specific MMP inhibitors [39]. Five drugs designed to target MMP have been studied for AIS/ICH (Table 1). As promising candidates of MMP-9 inhibitors, mAbs are capable of distinguishing two or more closely related protease family members [40–44]. In addition, mAb has advantages in stability and half-life in blood than small-molecule agents [45–47]. In this study, MMP-9 mAb L13, isolated from an inhibitory function-based strategy, was validated for its therapeutic effects for treating both ischemic and hemorrhagic strokes. Compared to the previously reported MMP-9 mAb with only prophylactic effect on ischemic stroke [23,24], L13 is up to now the first MMP-9 neutralizing antibody with clear therapeutic potential and mechanism of action for both ischemic and hemorrhagic stroke treatments. In order to compare the efficacy of L13 with currently available MMP9 inhibitors, we selected SB-3CT, the most-specific MMP-9 inhibitors reported so far, which actually has higher binding affinities to MMP-2 than MMP-9 [21]. SB-3CT has been widely used in animal stroke studies with well-established dosage regimen and efficacy [32,33], thus can serve as a good positive control of L13 mAb. We compared the protective effects of L13 mAb and SB-3CT in a mouse model of ischemic stroke. Our results showed that L13 mAb achieved a similar protective effect to SC-3CT, in terms of infarct volume, neurological and motor functions. Given that L13 mAb has much higher specificity (Ki=120 nM for MMP9, no inhibition of MMP2/12/14) than SB-3CT (Ki=600 nM for MMP9, Ki=13.9 nM for MMP2) [21,25] and requires only one injection within days after stroke due to longer half-life of antibody drugs, we believe that L13 mAb has higher translational potential than current MMP9 small-molecule inhibitors for stroke treatment.

During acute stroke, in addition to MMP-9, several other MMPs are also reported to be upregulated in brain tissues. For example, MMP-2 was activated following ischemic and hemorrhagic stroke in animal models or patients [17,48–50]. In addition, upregulation of MMP-3/− 13 after cerebral ischemia and MMP-3/− 7/− 12 in intracerebral hemorrhage models were also previously observed [48,51,52]. This raises a question whether specific inhibition of MMP-9 *versus* simultaneous inhibition of multiple MMPs is the optimal strategy. However, concrete and consistent evidence has been lacking to support the roles of these MMPs other than MMP-9 in acute stroke. Based on previous studies, it appears that specific inhibition of MMP-9 in the early phase of acute stroke is a strategy with highest reliability, effectiveness and safety. Many studies including ours using *Mmp9* KO mice consistently showed neuro- and BBB-protective effects of *Mmp9* genetic deletion after ischemic stroke [14], whereas the results with other MMP KO animals such as MMP-2 have been controversial or unclear [53,54]. Meanwhile, previous studies showed that MMP-9 is the most abundantly increased MMPs in the acute stage after stroke, whereas MMP-2 is mainly increased at a later stage (several days) after stroke [48,49,55,56], suggesting that MMP-9 is responsible for acute brain tissue injury after stroke. Further, specific inhibition of MMP-9 other than simultaneous inhibition of multiple MMPs may reduce safety issues as MMPs are involved in many biological processes, some of which may be important for brain function during both the acute injury and chronic repair phase after stroke. Last but not least, the early timing of MMP-9 inhibition is critical to ensure beneficial outcomes as MMP-9 was reported to also play a role during the delayed cortical responses after stroke [57,58].

Similar to ischemic stroke, MMP-9 has been shown to be rapidly increased in mouse brain tissue and human serum after acute ICH [16]. However, the therapeutic effect of MMP-9 inhibition in ICH has been debatable. MMP inhibitors including GM6001, BB-1101 and minocycline significantly improved the outcomes of experimental ICH [17,18]. In contrast, studies also found that broad spectrum MMP inhibitor BB-94 or *Mmp9* genetic deletion showed deleterious effects in animal ICH models [19,20]. In the current study, we found no significant difference in hematoma volume and BBB leakage between *Mmp9* KO mice and WT mice (Supplementary Fig. 4), likely due to the compensatory upregulation of MMP-2/− 3 expression after long-term *Mmp9* deficiency [19]. Moreover, we found a beneficial effect of MMP-9 inhibition by L13 in the mouse ICH model, suggesting that the deleterious effects of pharmacological inhibition of MMP-9 seen by previous studies might result from the non-specific side effects of the broad MMP inhibitors used. Therefore, our results clearly demonstrated that exclusive and temporal inhibition of MMP-9 by L13 was able to improve the outcomes of ICH *via* protecting BBB by a mechanism similar to that in ischemic stroke.

The therapeutic time window for MMP-9 inhibition is critical to the success of stroke treatment. MMP-9 expression and activity are rapidly induced and upregulated within hours following either cerebral ischemia or intracerebral hemorrhage and reached the peak within 24–48 h [16,38,59]. Therefore, we speculated that implementation of MMP-9 inhibition *via* L13 as early as possible would incur the maximal BBB-protective effect. Indeed, a previous study using the MMP-2/9 dual inhibitor SB-3CT has demonstrated that MMP-9 inhibition was effective to reduce infarct volume of mice when the treatment was implemented before or within 6 h of the onset of 2-h cerebral ischemia, but was ineffective when the treatment was implemented at 10 h after the onset of 2-h cerebral ischemia [32], suggesting a narrow therapeutic window for MMP-9 inhibition in stroke treatment. On the basis of these previous studies, we administered L13 at the onset of reperfusion or after collagenase VII injection in the ICH model, and observed encouraging therapeutic effects in both stroke models. Furthermore, our unpublished data shown that the half-life of intravenously injected L13 was around 4–5 days. Therefore, the administration of L13 immediately after the onset of stroke can cover most of the acute stage of stroke when MMP-9 is upregulated and detrimental, but would not affect the important beneficial role of MMP-9 in delayed cortical responses after stroke (> 7days) [58].

In order to provide more direct evidence of L13 for the treatment of stroke in clinic, we determined the neutralizing effect of L13 on human MMP-9 activity in serum or brain tissue samples of stroke patients, which can be recognized as a small-scale *ex vivo* clinical trial. Serum levels of MMP-9 in patients with acute stroke is positively correlated with BBB damage and prognosis [60–63]. Therefore, the inhibitory effect of L13 on MMP-9 in serum and brain tissue samples of stroke patients *ex vivo* can conceivably reflect the therapeutic potential of L13 on MMP-9 related brain injury in stroke patients. We found that the MMP-9 protein level in ICH patients was higher than that in healthy adults, but there was no significant difference between AIS patients and healthy adults. In a previous clinical study [64], the serum MMP-9 levels of AIS patients were higher than that of healthy control group, which is inconsistent with our data possibly because that we collected samples within 24 h after AIS onset, which maybe not the time point when MMP-9 is abundantly secreted into the blood after AIS. Another possible reason is that Western blot analysis was not sensitive enough for detecting differences of serum MMP-9 as compared with ELISA. However, gelatin zymography assay was sensitive enough to show that MMP-9 activities were significantly decreased by L13 treatment in both AIS and ICH patients. More importantly, the MMP-9 activity in the peri-hematoma brain tissues of ICH patients was also substantially reduced by L13 treatment. Our data provide direct evidence that L13

may be clinically effective in the treatment of stroke patients.

Last but not least, the effects of MMP-9 inhibition on other comorbidities in stroke patients should be considered. Stroke is often associated with other comorbidities in aged population, such as obesity, diabetes, hypertension, *etc.* Increased levels of MMP-9 have been widely found in a variety of cardio-metabolic diseases, chronic kidney disease, and cancers, and may play important roles in the pathogenesis of these diseases [65–67]. Investigations are needed to determine how short-term administration of MMP-9 neutralizing antibodies during the acute stage of stroke would affect these co-existing diseases in stroke patients.

## 5. Conclusion

Overall, our findings describe a highly promising human mAb drug and demonstrate that neutralizing mAbs that exclusively target MMP-9 constitute a potential feasible therapeutic approach for both ischemic and hemorrhagic stroke. Further clinical trials are needed to explore the safety and efficacy of L13 in stroke patients.

## CRediT authorship contribution statement

J.C. and F.G. conceived and supervised the study. Y.J., Q.G., Y.M., F. W. and D.S. performed the *in vivo* experiments. Y.J. performed the *in vitro* experiments. Z.W. and X.G. prepared the L13 mAb. F.G., H.H., Y.J. and X.T. collected samples of stroke patients. Y.J., J.C., F.G., Q.G. and Y. M. analyzed the data and wrote the manuscript. X.G. and R.H. commented on the manuscript. All authors read and approved the final manuscript.

## Conflict of interest

The authors declare no conflict of interest.

## Data availability

Data will be made available on request.

## Acknowledgments

This study was supported by the National Natural Science Foundation of China (32170985, 81771293), National Key R&D Program of China (2021YFE0204700, 2021YFA0910000), the Guangdong Basic and Applied Basic Research Foundation, China (2021B1515120089, 2021A1515220105), Science Technology and Innovation Commission of Shenzhen Municipality (JCYJ20200109114608075, JCYJ20210324115800003, SGLH20180625142404672), International collaboration project of Chinese Academy of Sciences (172644KYSB20200045), CAS-Croucher Funding Scheme for Joint Laboratories, and Guangdong Innovation Platform of Translational Research for Cerebrovascular Diseases. The funders were not involved in study design, data collection, data analysis, manuscript preparation and/or publication decisions.

## Appendix A. Supporting information

Supplementary data associated with this article can be found in the online version at doi:10.1016/j.phrs.2023.106720.

## References

[1] C.P. Profaci, R.N. Munji, R.S. Pulido, R. Daneman, The blood-brain barrier in health and disease: important unanswered questions, J. Exp. Med 217 (4) (2020).
[2] M.D. Sweeney, K. Kisler, A. Montagne, A.W. Toga, B.V. Zlokovic, The role of brain vasculature in neurodegenerative disorders, Nat. Neurosci. 21 (10) (2018) 1318–1331.
[3] X. Jiang, A.V. Andjelkovic, L. Zhu, T. Yang, M.V.L. Bennett, J. Chen, R.F. Keep, Y. Shi, Blood-brain barrier dysfunction and recovery after ischemic stroke, Prog. Neurobiol. 163- 164 (2018) 144–171.
[4] S. Liebner, R.M. Dijkhuizen, Y. Reiss, K.H. Plate, D. Agalliu, G. Constantin, Functional morphology of the blood-brain barrier in health and disease, Acta Neuropathol. 135 (3) (2018) 311–336.
[5] R. Khatri, A.M. McKinney, B. Swenson, V. Janardhan, Blood-brain barrier, reperfusion injury, and hemorrhagic transformation in acute ischemic stroke, Neurology 79 (13 Suppl 1) (2012) S52–S57.
[6] J. Bai, P.D. Lyden, Revisiting cerebral postischemic reperfusion injury: new insights in understanding reperfusion failure, hemorrhage, and edema, Int. J. Stroke 10 (2) (2015) 143–152.
[7] R.F. Keep, A.V. Andjelkovic, J.M. Xiang, S.M. Stamatovic, D.A. Antonetti, Y. Hua, G.H. Xi, Brain endothelial cell junctions after cerebral hemorrhage: Changes, mechanisms and therapeutic targets, J. Cereb. Blood Flow. Metab. 38 (8) (2018) 1255–1275.
[8] L. Shi, M. Rocha, R.K. Leak, J. Zhao, T.N. Bhatia, H. Mu, Z. Wei, F. Yu, S.L. Weiner, F. Ma, T.G. Jovin, J. Chen, A new era for stroke therapy: Integrating neurovascular protection with optimal reperfusion, J Cereb Blood Flow Metab (2018) 271678×18798162.
[9] R. Wangqin, D.T. Laskowitz, Y.J. Wang, Z.X. Li, Y.L. Wang, L.P. Liu, L. Liang, R. A. Matsouaka, J.L. Saver, G.C. Fonarow, D.L. Bhatt, E.E. Smith, L.H. Schwamm, J. P. Bettger, A.F. Hernandez, E.D. Peterson, Y. Xian, International comparison of patient characteristics and quality of care for ischemic stroke: analysis of the china national stroke registry and the american heart association get with the guidelines-stroke program, J. Am. Heart Assoc. 7 (20) (2018).
[10] J. Montaner, L. Ramiro, A. Simats, M. Hernandez-Guillamon, P. Delgado, A. Bustamante, A. Rosell, Matrix metalloproteinases and ADAMs in stroke, Cell. Mol. life Sci.: CMLS 76 (16) (2019) 3117–3140.
[11] R.G. Rempe, A.M.S. Hartz, B. Bauer, Matrix metalloproteinases in the brain and blood-brain barrier: versatile breakers and makers, J. Cereb. Blood Flow. Metab. 36 (9) (2016) 1481–1507.
[12] Y. Yang, G.A. Rosenberg, Matrix metalloproteinases as therapeutic targets for stroke, Brain Res. 2015 (1623) 30–38.
[13] M. Asahi, X. Wang, T. Mori, T. Sumii, J.C. Jung, M.A. Moskowitz, M.E. Fini, E. H. Lo, Effects of matrix metalloproteinase-9 gene knock-out on the proteolysis of blood-brain barrier and white matter components after cerebral ischemia, J. Neurosci. 21 (19) (2001), 7724-32.
[14] M. Chaturvedi, L. Kaczmarek, Mmp-9 inhibition: a therapeutic strategy in ischemic stroke, Mol. Neurobiol. 49 (1) (2014) 563–573.
[15] B. Vafadari, A. Salamian, L. Kaczmarek, MMP-9 in translation: from molecule to brain physiology, pathology, and therapy, J. Neurochem 139 (Suppl 2) (2016) 91–114.
[16] S. Lattanzi, M. Di Napoli, S. Ricci, A.A. Divani, Matrix Metalloproteinases in Acute Intracerebral Hemorrhage, Neurotherapeutics 17 (2) (2020) 484–496.
[17] G.A. Rosenberg, M. Navratil, Metalloproteinase inhibition blocks edema in intracerebral hemorrhage in the rat, Neurology 48 (4) (1997) 921–926.
[18] J. Wang, S.E. Tsirka, Neuroprotection by inhibition of matrix metalloproteinases in a mouse model of intracerebral haemorrhage, Brain 128 (Pt 7) (2005), 1622-33.
[19] J. Tang, J. Liu, C. Zhou, J.S. Alexander, A. Nanda, D.N. Granger, J.H. Zhang, Mmp-9 deficiency enhances collagenase-induced intracerebral hemorrhage and brain injury in mutant mice, J. Cereb. Blood Flow. Metab. 24 (10) (2004) 1133–1145.
[20] M. Grossetete, G.A. Rosenberg, Matrix metalloproteinase inhibition facilitates cell death in intracerebral hemorrhage in mouse, J. Cereb. Blood Flow. Metab. 28 (4) (2008) 752–763.
[21] S. Brown, M.M. Bernardo, Z.H. Li, L.P. Kotra, Y. Tanaka, R. Fridman, S. Mobashery, Potent and selective mechanism-based inhibition of gelatinases, J. Am. Chem. Soc. 122 (28) (2000) 6799–6800.
[22] W. Song, Z. Peng, M. Gooyit, M.A. Suckow, V.A. Schroeder, W.R. Wolter, M. Lee, M. Ikejiri, J. Cui, Z. Gu, M. Chang, Water-soluble mmp-9 inhibitor prodrug generates active metabolites that cross the blood-brain barrier, ACS Chem. Neurosci. 4 (8) (2013) 1168–1173.
[23] N. Ramos-DeSimone, U.M. Moll, J.P. Quigley, D.L. French, Inhibition of matrix metalloproteinase 9 activation by a specific monoclonal antibody, Hybridoma 12 (4) (1993) 349–363.
[24] A.M. Romanic, R.F. White, A.J. Arleth, E.H. Ohlstein, F.C. Barone, Matrix metalloproteinase expression increases after cerebral focal ischemia in rats: inhibition of matrix metalloproteinase-9 reduces infarct size, Stroke 29 (5) (1998) 1020–1030.
[25] T. Lopez, Z. Mustafa, C. Chen, K.B. Lee, A. Ramirez, C. Benitez, X. Luo, R.R. Ji, X. Ge, Functional selection of protease inhibitory antibodies, Proc. Natl. Acad. Sci. USA 116 (33) (2019) 16314–16319.
[26] T. Chiang, R.O. Messing, W.H. Chou, Mouse model of middle cerebral artery occlusion, J. Vis. Exp. 48 (2011).
[27] A.J. Hunter, J. Hatcher, D. Virley, P. Nelson, E. Irving, S.J. Hadingham, A. A. Parsons, Functional assessments in mice and rats after focal stroke, Neuropharmacology 39 (5) (2000) 806–816.
[28] F. Yonemori, T. Yamaguchi, H. Yamada, A. Tamura, Evaluation of a motor deficit after chronic focal cerebral ischemia in rats, J. Cereb. Blood Flow. Metab. 18 (10) (1998) 1099–1106.
[29] G.A. Metz, I.Q. Whishaw, Cortical and subcortical lesions impair skilled walking in the ladder rung walking test: a new task to evaluate fore- and hindlimb stepping, placing, and co-ordination, J. Neurosci. Methods 115 (2) (2002) 169–179.
[30] Y.B. Ji, Y.M. Wu, Z. Ji, W. Song, S.Y. Xu, Y. Wang, S.Y. Pan, Interrupted intracarotid artery cold saline infusion as an alternative method for neuroprotection after ischemic stroke, Neurosurg. Focus 33 (1) (2012).

[31] Y.B. Ji, Q. Gao, X.X. Tan, X.W. Huang, Y.Z. Ma, C. Fang, S.N. Wang, L.H. Qiu, Y. X. Cheng, F.Y. Guo, J. Chang, Lithium alleviates blood-brain barrier breakdown after cerebral ischemia and reperfusion by upregulating endothelial Wnt/beta-catenin signaling in mice, Neuropharmacology 186 (2021), 108474.
[32] Z.Z. Gu, J. Cui, S. Brown, R. Fridman, S. Mobashery, A.Y. Strongin, S.A. Lipton, A highly specific inhibitor of matrix metalloproteinase-9 rescues laminin from proteolysis and neurons from apoptosis in transient focal cerebral ischemia, J. Neurosci. 25 (27) (2005) 6401–6408.
[33] B. Liao, L. Geng, F. Zhang, L. Shu, L. Wei, P.K.K. Yeung, K.S.L. Lam, S.K. Chung, J. Chang, P.M. Vanhoutte, A. Xu, K. Wang, R.L.C. Hoo, Adipocyte fatty acid-binding protein exacerbates cerebral ischaemia injury by disrupting the blood-brain barrier, Eur. Heart J. 41 (33) (2020) 3169–3180.
[34] D. Knowland, A. Arac, K.J. Sekiguchi, M. Hsu, S.E. Lutz, J. Perrino, G.K. Steinberg, B.A. Barres, A. Nimmerjahn, D. Agalliu, Stepwise recruitment of transcellular and paracellular pathways underlies blood-brain barrier breakdown in stroke, Neuron 82 (3) (2014) 603–617.
[35] B. Dang, X. Duan, Z. Wang, W. He, G. Chen, A. Therapeutic, Target of cerebral hemorrhagic stroke: matrix metalloproteinase- 9, Curr. Drug Targets 18 (12) (2017) 1358–1366.
[36] C. Cordonnier, A. Demchuk, W. Ziai, C.S. Anderson, Intracerebral haemorrhage: current approaches to acute management, Lancet 392 (10154) (2018) 1257–1268.
[37] W. Stocker, F. Grams, U. Baumann, P. Reinemer, F.X. Gomisruth, D.B. Mckay, W. Bode, The Metzincins - Topological and Sequential Relations between the Astacins, Adamalysins, Serralysins, and Matrixins (Collagenases) Define a Superfamily of Zinc-Peptidases, Protein Sci. 4 (5) (1995) 823–840.
[38] M. Asahi, K. Asahi, J.C. Jung, G.J. del Zoppo, M.E. Fini, E.H. Lo, Role for matrix metalloproteinase 9 after focal cerebral ischemia: effects of gene knockout and enzyme inhibition with BB-94, J. Cereb. Blood Flow. Metab. 20 (12) (2000) 1681–1689.
[39] Y. Li, W. Zhong, Z. Jiang, X. Tang, New progress in the approaches for blood-brain barrier protection in acute ischemic stroke, Brain Res. Bull. 144 (2019) 46–57.
[40] Y. Wu, C. Eigenbrot, W.C. Liang, S. Stawicki, S. Shia, B. Fan, R. Ganesan, M. T. Lipari, D. Kirchhofer, Structural insight into distinct mechanisms of protease inhibition by antibodies, Proc. Natl. Acad. Sci. USA 104 (50) (2007) 19784–19789.
[41] L. Devy, L. Huang, L. Naa, N. Yanamandra, H. Pieters, N. Frans, E. Chang, Q. Tao, M. Vanhove, A. Lejeune, R. van Gool, D.J. Sexton, G. Kuang, D. Rank, S. Hogan, C. Pazmany, Y.L. Ma, S. Schoonbroodt, A.E. Nixon, R.C. Ladner, R. Hoet, P. Henderikx, C. Tenhoor, S.A. Rabbani, M.L. Valentino, C.R. Wood, D. T. Dransfield, Selective inhibition of matrix metalloproteinase-14 blocks tumor growth, invasion, and angiogenesis, Cancer Res. 69 (4) (2009) 1517–1526.
[42] E.L. Schneider, M.S. Lee, A. Baharuddin, D.H. Goetz, C.J. Farady, M. Ward, C. I. Wang, C.S. Craik, A reverse binding motif that contributes to specific protease inhibition by antibodies, J. Mol. Biol. 415 (4) (2012) 699–715.
[43] J.A. Kenniston, R.R. Faucette, D. Martik, S.R. Comeau, A.P. Lindberg, K.J. Kopacz, G.P. Conley, J. Chen, M. Viswanathan, N. Kastrapeli, J. Cosic, S. Mason, M. DiLeo, J. Abendroth, P. Kuzmic, R.C. Ladner, T.E. Edwards, C. TenHoor, B.A. Adelman, A. E. Nixon, D.J. Sexton, Inhibition of plasma kallikrein by a highly specific active site blocking antibody, J. Biol. Chem. 289 (34) (2014) 23596–23608.
[44] D.H. Nam, C. Rodriguez, A.G. Remacle, A.Y. Strongin, X. Ge, Active-site MMP-selective antibody inhibitors discovered from convex paratope synthetic libraries, Proc. Natl. Acad. Sci. USA 113 (52) (2016) 14970–14975.
[45] Y.J. Yu, J.K. Atwal, Y. Zhang, R.K. Tong, K.R. Wildsmith, C. Tan, N. Bien-Ly, M. Hersom, J.A. Maloney, W.J. Meilandt, D. Bumbaca, K. Gadkar, K. Hoyte, W. Luk, Y. Lu, J.A. Ernst, K. Scearce-Levie, J.A. Couch, M.S. Dennis, R.J. Watts, Therapeutic bispecific antibodies cross the blood-brain barrier in nonhuman primates, Sci. Transl. Med. 6 (261) (2014) 261ra154.
[46] S.K. Sharma, K.D. Bagshawe, Antibody directed enzyme prodrug therapy (ADEPT): trials and tribulations, Adv. Drug Deliv. Rev. 118 (2017) 2–7.
[47] X. Wang, M. Mathieu, R.J. Brezski, IgG Fc engineering to modulate antibody effector functions, Protein Cell 9 (1) (2018) 63–73.
[48] C. Power, S. Henry, M.R. Del Bigio, P.H. Larsen, D. Corbett, Y. Imai, V.W. Yong, J. Peeling, Intracerebral hemorrhage induces macrophage activation and matrix metalloproteinases, Ann. Neurol. 53 (6) (2003) 731–742.
[49] A.M. Planas, S. Sole, C. Justicia, Expression and activation of matrix metalloproteinase-2 and -9 in rat brain after transient focal cerebral ischemia, Neurobiol. Dis. 8 (5) (2001) 834–846.
[50] A.W. Clark, C.A. Krekoski, S.S. Bou, K.R. Chapman, D.R. Edwards, Increased gelatinase A (MMP-2) and gelatinase B (MMP-9) activities in human brain after focal ischemia, Neurosci. Lett. 238( (1–2) (1997) 53–56.
[51] E. Cuadrado, A. Rosell, M. Borrell-Pages, L. Garcia-Bonilla, M. Hernandez-Guillamon, A. Ortega-Aznar, J. Montaner, Matrix metalloproteinase-13 is activated and is found in the nucleus of neural cells after cerebral ischemia, J. Cereb. Blood Flow. Metab. 29 (2) (2009) 398–410.
[52] S. Sole, V. Petegnief, R. Gorina, A. Chamorro, A.M. Planas, Activation of matrix metalloproteinase-3 and agrin cleavage in cerebral ischemia/reperfusion, J. Neuropathol. Exp. Neurol. 63 (4) (2004) 338–349.
[53] M. Asahi, T. Sumii, M.E. Fini, S. Itohara, E.H. Lo, Matrix metalloproteinase 2 gene knockout has no effect on acute brain injury after focal ischemia, Neuroreport 12 (13) (2001) 3003–3007.
[54] A. Lu, Y. Suofu, F. Guan, J.P. Broderick, K.R. Wagner, J.F. Clark, Matrix metalloproteinase-2 deletions protect against hemorrhagic transformation after 1h of cerebral ischemia and 23h of reperfusion, Neuroscience 253 (2013) 361–367.
[55] J.H. Heo, J. Lucero, T. Abumiya, J.A. Koziol, B.R. Copeland, G.J. del Zoppo, Matrix metalloproteinases increase very early during experimental focal cerebral ischemia, J. Cereb. Blood Flow. Metab. 19 (6) (1999) 624–633.
[56] Y. Gasche, M. Fujimura, Y. Morita-Fujimura, J.C. Copin, M. Kawase, J. Massengale, P.H. Chan, Early appearance of activated matrix metalloproteinase-9 after focal cerebral ischemia in mice: a possible role in blood-brain barrier dysfunction, J. Cereb. Blood Flow. Metab. 19 (9) (1999) 1020–1028.
[57] Y. Yang, J.F. Thompson, S. Taheri, V.M. Salayandia, T.A. McAvoy, J.W. Hill, Y. R. Yang, E.Y. Estrada, G.A. Rosenberg, Early inhibition of MMP activity in ischemic rat brain promotes expression of tight junction proteins and angiogenesis during recovery, J Cerebr Blood F, Met 33 (7) (2013) 1104–1114.
[58] B.Q. Zhao, S. Wang, H.Y. Kim, H. Storrie, B.R. Rosen, D.J. Mooney, X. Wang, E. H. Lo, Role of matrix metalloproteinases in delayed cortical responses after stroke, Nat. Med 12 (4) (2006) 441–445.
[59] M. Fujimura, Y. Gasche, Y. Morita-Fujimura, J. Massengale, M. Kawase, P.H. Chan, Early appearance of activated matrix metalloproteinase-9 and blood-brain barrier disruption in mice after focal cerebral ischemia and reperfusion, Brain Res 842 (1) (1999) 92–100.
[60] J. Montaner, C.A. Molina, J. Monasterio, S. Abilleira, J.F. Arenillas, M. Ribo, M. Quintana, J. Alvarez-Sabin, Matrix metalloproteinase-9 pretreatment level predicts intracranial hemorrhagic complications after thrombolysis in human stroke, Circulation 107 (4) (2003) 598–603.
[61] J. Montaner, J. Alvarez-Sabin, C.A. Molina, A. Angles, S. Abilleira, J. Arenillas, J. Monasterio, Matrix metalloproteinase expression is related to hemorrhagic transformation after cardioembolic stroke, Stroke 32 (12) (2001) 2762–2767.
[62] J. Montaner, J. Alvarez-Sabin, C. Molina, A. Angles, S. Abilleira, J. Arenillas, M. A. Gonzalez, J. Monasterio, Matrix metalloproteinase expression after human cardioembolic stroke: temporal profile and relation to neurological impairment, Stroke 32 (8) (2001) 1759–1766.
[63] D. Petrovska-Cvetkovska, N. Dolnenec-Baneva, D. Nikodijevik, T. Chepreganova-Changovska, Correlative study between serum matrix metalloproteinase-9 values and neurologic deficit in acute, primary, supratentorial, intracerebral haemorrhage, Pril. (Make Akad. Nauk. Umet. Odd. Med Nauk. ) 35 (2) (2014) 39–44.
[64] S. Horstmann, P. Kalb, J. Koziol, H. Gardner, S. Wagner, Profiles of matrix metalloproteinases, their inhibitors, and laminin in stroke patients: influence of different therapies, Stroke 34 (9) (2003) 2165–2170.
[65] G. Caimi, E. Hopps, M. Montana, C. Urso, C. Carollo, B. Canino, R. Lo, Presti, The function of matrix metalloproteinase-9 (MMP-9) and its tissue inhibitor (TIMP-1) in several clinical conditions: Results and analysis of our survey, Clin. Hemorheol. Micro 78 (4) (2021) 401–416.
[66] J. Wozniak, J. Floege, T. Ostendorf, A. Ludwig, Key metalloproteinase-mediated pathways in the kidney, Nat. Rev. Nephrol. 17 (8) (2021) 513–527.
[67] K. Augoff, A. Hryniewicz-Jankowska, R. Tabola, K. Stach, MMP9: a tough target for targeted therapy for cancer, cancers (Basel) 14 (7) (2022).
[68] R.R. Sood, S. Taheri, E. Candelario-Jalil, E.Y. Estrada, G.A. Rosenberg, Early beneficial effect of matrix metalloproteinase inhibition on blood-brain barrier permeability as measured by magnetic resonance imaging countered by impaired long-term recovery after stroke in rat brain, J. Cereb. Blood Flow. Metab. 28 (2) (2008) 431–438.
[69] Y. Yang, E.Y. Estrada, J.F. Thompson, W. Liu, G.A. Rosenberg, Matrix metalloproteinase-mediated disruption of tight junction proteins in cerebral vessels is reversed by synthetic matrix metalloproteinase inhibitor in focal ischemia in rat, J. Cereb. Blood Flow. Metab. 27 (4) (2007) 697–709.
[70] Y. Yang, J.F. Thompson, S. Taheri, V.M. Salayandia, T.A. McAvoy, J.W. Hill, Y. Yang, E.Y. Estrada, G.A. Rosenberg, Early inhibition of MMP activity in ischemic rat brain promotes expression of tight junction proteins and angiogenesis during recovery, J. Cereb. Blood Flow. Metab. 33 (7) (2013) 1104–1114.